Palaeobiodiversity and Palaeoenvironments (2024) 104:1–28
https://doi.org/10.1007/s12549-023-00586-y

SENCKENBERG

ORIGINAL PAPER

Early Paleogene precipitation patterns over East Asia: Was there a monsoon after all?

Olesia V. Bondarenko[1] · **Torsten Utescher**[2,3]

Received: 19 December 2022 / Revised: 25 April 2023 / Accepted: 28 June 2023 / Published online: 8 September 2023

Abstract

Early Paleogene latitudinal precipitation gradients and patterns along the Pacific coast of Eurasia are studied in time and space using the Coexistence Approach, for the first time applied on an extensive regional palaeobotanical record. The palaeobotanical data used in this reconstruction are compiled from literature resources on 110 reasonably well-dated floras, including terrestrial deposits of 73 sites located in the Far East of Russia, Eastern Siberia, China, and Japan, and covering the early Palaeocene to early Eocene. Our reconstructions of precipitation for the Pacific side of Eurasia in the early Paleogene demonstrate a clear division (especially pronounced in the early Eocene) into two zones at ca. 50° N palaeolatitude on all precipitation parameters. Our results reveal very weak latitudinal precipitation gradients during the early and late Palaeocene. In the early Eocene, the gradient became more clearly pronounced, and a larger "arid" zone can be distinguished in the mid-latitudes. Our data suggest that in the early Paleogene, the global atmospheric circulation consisted of two well-defined cells, Hadley and Ferrell, while the polar cell was either absent or located over the Arctic Ocean and was very weak. Based on our reconstructions, the records could not be interpreted in terms of a monsoonal type of climate. The regional distribution of hygrophilous and xerophilous taxa in our early Eocene record largely coincides with the reconstructed precipitation pattern and generally corresponds to the distribution of coals and/or oil shales and red beds and/or evaporites, respectively.

Keywords Coexistence Approach · Spatial precipitation gradient · Temporal climatic trends · Precipitation seasonality · Monsoon · Global atmospheric circulation

Introduction

Eurasia is the largest continent of the planet, spanning a wide range of climate types. In addition, Eurasia is the northernmost continent of the planet, the climate of which was the most dynamic due to the cold spreading from the pole. Today the main feature of the climate of Eurasia is diversity because of the considerable longitudinal extent of the continent. Eurasian climate is characterised by a distinct contrast between the western (Atlantic) and eastern (Pacific) side, with a central region marked by strong seasonality typical of continental interiors (Rhines and Hakinnen 2003; Takaya and Nakamura 2005). Moreover, the Eurasian climate is strongly impacted by the surrounding oceans causing an asymmetric distribution of Koeppen–Geiger climate types over the continent (Fig. 1a; Kottek et al. 2006). The Atlantic Ocean, due to western transfer in mid- latitudes, humidifies the climate of Europe and even Siberia. Past climates of westerm Eurasia reflect various states of the North Atlantic Ocean circulation system and changes in the intensity of the Westerlies (e.g. Krapp and Jungclaus 2011) while coastal areas of eastern Eurasia mirror the varying intensity of the warm Kuroshio and cold, subarctic currents (e.g. Matthiessen et al. 2009). In eastern Eurasia, climate and prevailing precipitation patterns are connected to the history of the East Asian Monsoon System, complicated by tectonic movements and a shifting palaeogeography (e.g. An et al. 2001) (Fig. 1b).

At present, east Asian coastal areas, located in the transitional zone "continent-ocean", constantly experience the

✉ Torsten Utescher
torsten.utescher@senckenberg.de; t.utescher@uni-bonn.de

Olesia V. Bondarenko
laricioxylon@gmail.com

[1] Federal Scientific Center of the East Asia Terrestrial Biodiversity, Far Eastern Branch, Russian Academy of Sciences, Prospect Stoletiya 159, Vladivostok 690022, Russia

[2] Senckenberg Research Institute and Natural Museum, Senckenberganlage 25, 60325 Frankfurt M., Germany

[3] Institute for Geosciences, University of Bonn, Nussallee 8, 53115 Bonn, Germany

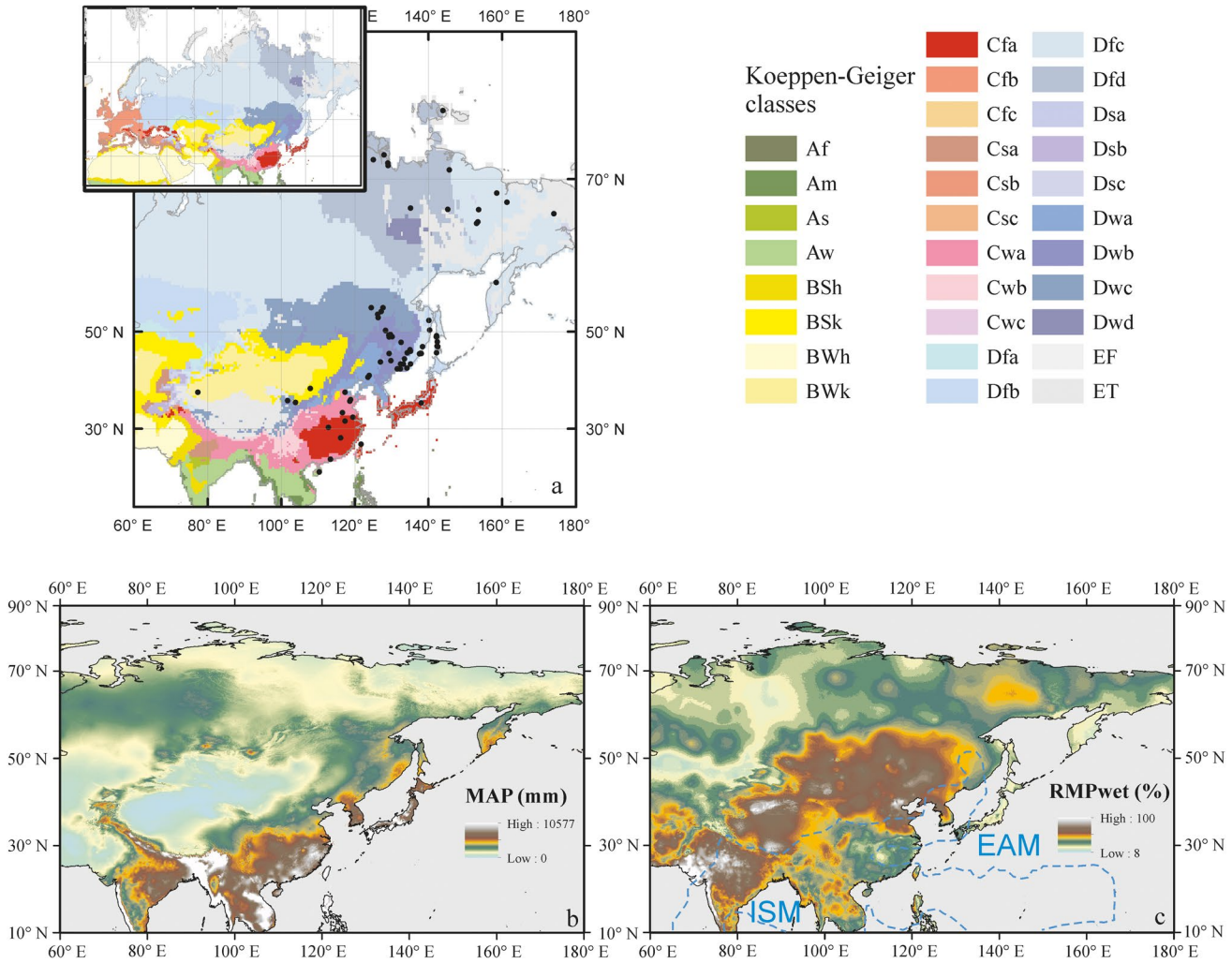

Fig. 1. Maps showing the early Paleogene sites in the context of modern Koeppen–Geiger type climates of Eurasia (**a**), modern MAP (**b**) and RMPwet (**c**) (calculated from WorldClim datasets). Koeppen-Geiger acronyms: *A* equatorial, *B* arid (*BS* steppe; *BW* desert), *C* warm temperate (megathermal), *D* snow climates (microthermal), *E* polar (*ET* tundra, *EF* frost); *w* winterdry, *s* summerdry, *f* fully humid, *m* monsoon, *h* hot, *k* cold. Additional qualifiers (in C and D climates): **a** hot summer, **b** warm summer, **c** cold summer and cold winter, **d** extremely continental. The dotted line on the RMPwet map refers to the demarcation of the major monsoon rainy season domains (National Centers for Environmental Prediction (NCEP); from Kalnay et al. (1996)

influence of oceanic-atmospheric and continental-atmospheric events. Thus, the study of the climate evolution of the Pacific side of Eurasia in the geological past, in particular in the early Paleogene, promotes the understanding of the formation of modern climate in this region.

Generally, the early Paleogene (Palaeocene – early Eocene) climate is characterised as being in a generally warm and equable "greenhouse" state across the world, punctuated by brief hyperthermal phases (Pagani et al. 2005; Dupont-Nivet et al. 2007; Zachos et al. 2008; Pearson et al. 2009; Xiao et al. 2010; Abels et al. 2011; Westerhold et al. 2020). At the same time, the evolution of Paleogene climates in eastern Eurasia is tied to the history of the warm Arctic (e.g. Spicer and Parrish 1986; Spicer and Corfield 1992; Herman and Spicer 1996, 1997; Amiot et al. 2004; Spicer and Herman 2010; Herman et al. 2016; Suan et al. 2017; Spicer et al. 2019; Bondarenko et al. 2022; Bondarenko and Utescher 2023), the development of the Okhotsk Sea (Semakin et al. 2016), India–Eurasia collision (Q. Zhang et al. 2012; An et al. 2021; Sehsah et al. 2022), the East Asian Monsoon (EAM) and it is further complicated by tectonic events such as uplift of the Tibetan Plateau, and the Sea of Japan back-arc opening (e.g. Kutzbach et al. 1989, 1993; Liu and Yin 2002; Akhmetiev 2004, 2015; Pavlyutkin and Golozubov 2010; Quan et al. 2012a, b; Liu et al. 2015; Akhmetiev and Zaporozhets 2017; Chen et al. 2022; Li et al. 2022).

Paleogene regional climates can be reconstructed from palaeobotanical records with different degrees of reliability,

depending on the spatio-temporal resolution of the palaeobotanical sites, and the taxonomic resolution of the studied plant organs (Akhmetiev 2004). The evolution of continental Paleogene climates has been well studied on the basis of palaeobotanical data from Australia, Europe, and North America (Greenwood and Wing 1995; Wilf 2000; Wing and Harrington 2001; Jolley and Widdowson 2005; Mosbrugger et al. 2005; Wing et al. 2005; Utescher et al. 2007, 2011; Greenwood et al. 2010) and marine proxy data from both hemispheres (Pearson et al. 2007; Zachos et al. 2008; Bijl et al. 2009). In East Asia, quantitative Paleogene climatic reconstructions on the basis of palaeobotanical data have been conducted on individual sites of China (e.g. He and Tao 1997; Quan and Zhang 2005; Su et al. 2009; Hao et al. 2010; Wang et al. 2010; Hoorn et al. 2012; Quan et al. 2012a, b; Chen et al. 2022). The comparison of the Cenozoic continental climate evolution from the Atlantic and Pacific side of Eurasia reveals the existence of differing regional patterns and spatial gradients from west to east, also in the past (Utescher et al. 2015). Recently, continental temperature patterns and gradients from south to north of East Asia in the early Paleogene have been studied in detail (Bondarenko and Utescher 2022). However, a detailed analysis of spatial precipitation patterns and gradients has not yet been performed.

The present-day monsoon systems impacting eastern Asia comprise the EAM and the South Asian Monsoon (SAM). The monsoons have clear differences (Molnar et al. 2010). The SAM is characterised by dry winters and wet summers, with temperatures being highest in May to early June, before the onset of the rainy season (Molnar et al. 2010). The EAM is characterised by cold and dry conditions in the cold season evolving under the influence of the Siberian High and affecting large parts of eastern Asia, and a warm and wet season setting in late spring to early summer when a low pressure cell forms over Siberia allowing the advection of moist air from the south (Molnar et al. 2010). At present, both systems affect different parts of Asia. The SAM mainly influences northern India and the northeastern Indian Ocean, while the EAM is mainly confined to China, the Korean Peninsula, and southern Japan (Molnar et al. 2010). EAM and SAM are also driven by specific orographic factors that cause specific precipitation patterns, not entirely understood so far. Moreover, the monsoonal character of the EAM has been questioned (for more details cf. Spicer et al. (2016) and Farnsworth et al. (2019) and discussions therein).

The evolution of the Asian monsoon systems throughout earth's history, and the causes of changes in SAM and EAM intensities, are still poorly understood (Spicer et al. 2019), although numerous studies were conducted to reconstruct the evolutionary history of the Asian monsoon circulation (e.g. An et al. 2001; Wan et al. 2007; Passey et al. 2009; Spicer et al. 2016, 2019; Bhatia et al. 2021a, 2022). According to Spicer et al (2016), no commonly applicable proxy is available so far to measure past monsoon intensity, due to the complexity of the drivers involved.

However, the palaeoclimatologists have also synthesized global monsoon variability from a geological perspective (An 2000; Wang 2009; Clemens et al. 2010; Ziegler et al. 2010; Caley et al. 2011; Cheng et al. 2012; An et al. 2015). Modelling and geological evidence suggest that monsoon-like circulation patterns likely occurred during the late Paleozoic to early Mesozoic as a consequence of the Pangaean megacontinent (Kutzbach et al. 1989; Loope et al. 2001). Palaeomonsoon evolution during the Cenozoic has been inferred from early Palaeocene tropical rainforest fossils in Colorado (Johnson and Ellis 2002) and from the Eocene monsoon forest in central Australia (Greenwood 1996). The palaeomonsoon system in East Asia was probably established during the late Eocene and persisted during the late Oligocene to Early Miocene, with further development thereafter (Parrish et al. 1982; Zhou 1984; Gu and Renaut 1994; Sun and Wang 2005; Guo et al. 2008; Qiang et al. 2011; An et al. 2014).

To determine short-term variability of monsoon intensity different indices have been used that are partly based on climatic parameters (Parthasarathy et al. 1992; Liu and Yin 2002; Zhang and Wang 2008; Zhao et al. 2009) or derived from atmospheric circulation (Goswami et al. 1999; Wang and Fan 1999). However, their applicability to geological records is limited (Spicer et al., 2016). Therefore, other proxies have been applied such as loess-palaeosol successions, isotopic data (Licht et al. 2014), or the terrestrial fossil records (Srivastava et al. 2012; Xing et al. 2012; Shukla et al. 2014; West et al. 2015; Bhatia et al. 2021a, 2022). Because the proxies used for investigation of past monsoon intensity are less precise, individual monsoon systems such as EAM and SAM are hard to differentiate from each other (Spicer et al. 2016). Nevertheless, some attempts have been made to differentiate these monsoon systems, e.g. based on leaf physiognomy (Spicer et al. 2016; Bhatia et al. 2021a, b).

We reconstructed detailed temperature patterns (Bondarenko and Utescher 2022) based on the same set of floras used in this study, and now we focus on precipitation gradients and patterns along the Pacific coast of Eurasia in space and time to trace climate seasonality in the early Paleogene. We compiled published palaeobotanical sites from the Russian Far East (RFE), Eastern Siberia, China, and Japan (Fig. 2). Based on a total of 110 reasonably well-dated pollen and leaf floras of the Pacific side of Eurasia, coherent climatic data sets are presented for the first time for three stratigraphic levels, namely for the early Palaeocene, late Palaeocene, and early Eocene, covering the climate evolution over a time-span of ca. 25 myr, in total. All the climate data are reconstructed using a single approach (the Coexistence Approach – CA) applicable on every plant organ type. For the application of the CA, the published flora lists and

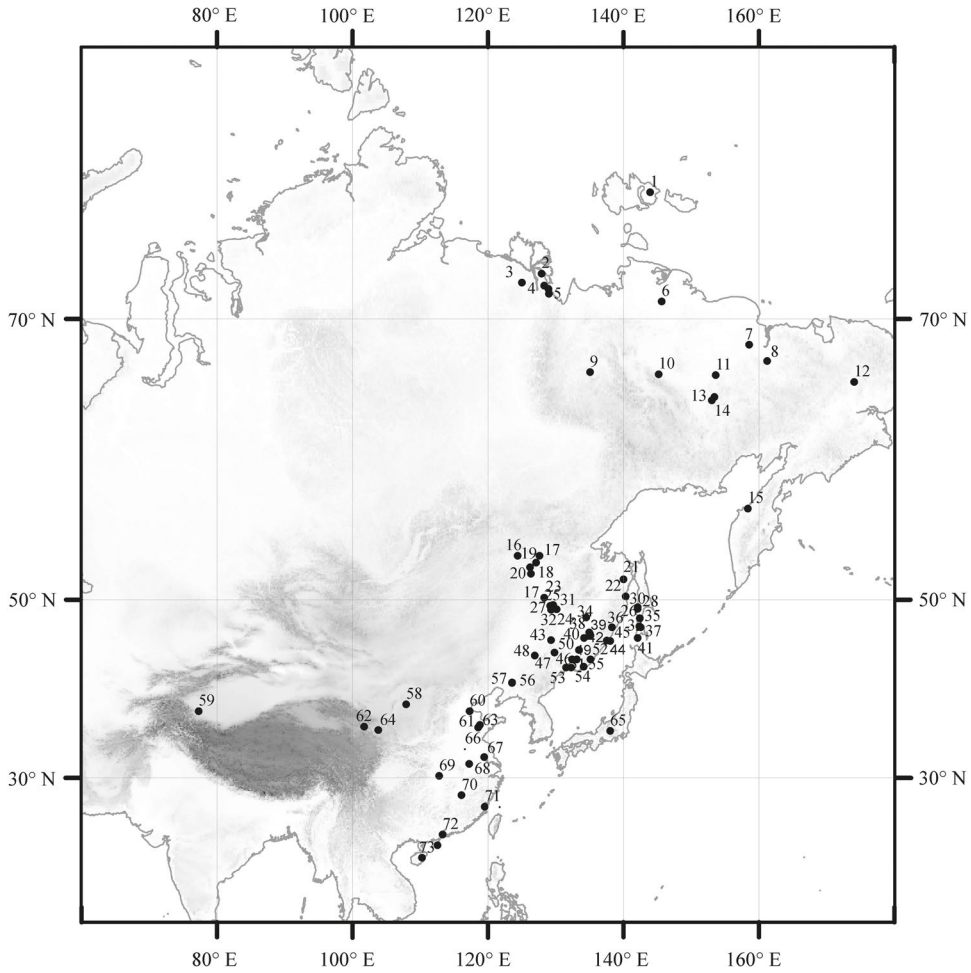

Fig. 2. Location of the selected early Paleogene sites of the Pacific side of Eurasia

Nearest Living Relative (NLR) interpretations of the fossil record were revisited and homogenized.

Materials and methods

The floral record

The palaeobotanical records of the Pacific part of Eurasia (including China, Japan, the RFE and Eastern Siberia) studied herein originate from 73 localities (Table 1, Fig. 2, ESM 1). Early Paleogene deposits are widely distributed in China and generally represent terrestrial facies conditions. The early Paleogene deposits of RFE and Eastern Siberia are also widely distributed and are likewise dominated by non-marine facies. For details on the Paleogene strata of the study area the reader is referred to Bondarenko and Utescher (2022).

We use regional stratigraphic schemes to allocate the palaeobotanical sites to a total of three time slices. The stratigraphic correlation chart provided in Electronic Supplementary Materials 1 (ESM 1) is combined from Quan et al. (2012a) for China, Kezina (2005) and Pavlyutkin and Petrenko (2010) for the continental part of the south RFE, Gladenkov et al. (2002) for Sakhalin Island, Gladenkov et al. (2005) for the Kamchatka Peninsula, and Grinenko et al. (1997) for the continental part of the north RFE and Eastern Siberia. Age control of the selected early Paleogene fossil floras of eastern Eurasia is based on a variety of stratigraphic data obtained from radiometric dating, well log correlations, and regional sequence-stratigraphical concepts, considering the position of volcanogenic units and main phases of peat formation, vertebrate fauna, mollusks, foraminifera, and regional and inter-regional pollen zonation (Table 1). The stratigraphic schemes of the RFE and Eastern Siberia have been tied to the International Stratigraphic Chart (Grinenko et al. 1997; Gladenkov et al. 2002, 2005; Kezina 2005; Pavlyutkin and Petrenko 2010; Cohen et al. 2013) and allow for dating the flora-bearing horizons at the stage level. For some of the floras, stratigraphic ages are constrained by radiometric dating (cf. ESM 1).

The palaeobotanical record of the Pacific coastal areas of Eurasia is diverse and has been subject to extensive taxonomic studies (cf. ESM 1 for references). In this study, all palaeofloras considered were carefully re-evaluated

Table 1. List of selected early Paleogene fossil sites of Eurasian Pacific side

Site	Location	Coordinate		Age control	PA	Formation/group (member)	Age	Fossil type	References
		Lat	Lon						
1	Novosibirskie Islands, Republic of Sakha, Russia	75°53'	143°91'	IRC, D, GD	1	Anzhuiskaya	EE	P, C	Fradkina (1995), Fradkina et al. (1979), Grinenko et al. (1989, 1997), Kulkova (1973), Suan et al. (2017)
2	Bykovskaya Channel, Republic of Sakha, Russia	72°20'	127°90'	IRC, D7	2	Kengdeiskaya	EE	P, L	Budantsev (1983), Fradkina (1995), Grinenko and Kiseleva (1971), Grinenko et al. (1989, 1997)
3	Kengdei, Republic of Sakha, Russia	71°79'	124°98'	IRC, Mo	3	Kengdeiskaya	EE	P, L	Fradkina (1995), Grinenko et al. (1989, 1997)
4	Sogo, Republic of Sakha, Russia	71°50'	128°90'	IRC	4	Soginskaya (upper part)	LP	P	Fradkina (1995), Grinenko et al. (1989, 1997)
				IRC	5	Soginskaya (lower part)	LP	P	Fradkina (1995), Grinenko and Fradkina (1988), Grinenko et al. (1989, 1997)
5	Kunga, Republic of Sakha, Russia	71°28'	128°99'	IRC, D	6	Kengdeiskaya	EE	P, L	Fradkina (1995), Grinenko et al. (1989, 1997), Laukhin et al. (1988)
				IRC	7	Emgend'enskaya	EE	P	Fradkina (1995), Grinenko et al. (1989, 1997)
6	Tastakh, Republic of Sakha, Russia	70°90'	145°60'	IRC	8	Tastakhskaya	EE	P, L	Budantsev (1983), Fradkina (1995), Krysh-tofovich (1958), Kulkova (1971, 1973)
7	Kolyma1, Republic of Sakha, Russia	68°70'	158°50'	IRC, SC	9	Timkinskaya	LP	P	Fradkina (1985, 1995), Fradkina and Laukhin (1984), Grinenko et al. (1989, 1997), Zharikova et al. (1982)
8	Yarovaya91, Chukotka Autonomous Region, Russia	67°80'	161°20'	IRC	10	Khetachanskaya (interval 84,0-160,8 m)	LP	P	Belaya and Litvinenko (1988), Fradkina (1995), Grinenko et al. (1997)
9	Diring-Yuryue15, Republic of Sakha, Russia	67°18'	135°07'	IRC, SC	11	Dirinskaya (interval 383-418 m)	EE	P	Fradkina (1995), Grinenko et al. (1989, 1997)
				IRC, SC	12	Yantarninskaya	LP	P	Fradkina (1995), Grinenko et al. (1989, 1997)
10	Sakan'ya272-1, Republic of Sakha, Russia	67°06'	145°20'	IRC	13	Sakan'inskaya (interval 832-1075 m)	EP	P	Fradkina (1995), Grinenko et al. (1997)
11	Slezovka15, Republic of Sakha, Russia	67°01'	153°60'	IRC, SC	14	Iryumasskaya	LP	P	Fradkina (1995), Grinenko et al. (1997)
				IRC	15	Afononskaya	EP	P	Fradkina (1995), Grinenko et al. (1997)
12	Koluchinskaya guba, Chukotka Autono-mous Region, Russia	66°60'	174°00'	IRC	16	Ukvyveemskaya	EP	P	Fradkina (1995), Grinenko et al. (1997), Kisterova et al. (1979), Volobueva et al. (1988)
13	Shamanikha, Republic of Sakha, Russia	65°70'	153°40'	IRC, SC	17	Shamanikhovskaya (upper part)	EE	P	Fradkina (1995), Grinenko et al. (1989), Zharikova (1980)
				IRC, SC	18	Shamanikhovskaya (lower part)	LP	P	Fradkina (1995), Grinenko et al. (1989), Zharikova (1980)
14	Medvezhye ozera, Republic of Sakha, Russia	65°50'	153°00'	IRC	19	Kopachskaya	EE	P	Fradkina (1995), Grinenko et al. (1989, 1997), Zharikova (1980)

Table 1. (continued)

Site	Location	Coordinate		Age control	PA	Formation/group (member)	Age	Fossil type	References
		Lat	Lon						
15	Tigil', Kamtchatka Peninsular, Russia	57,98	158,34	IRC	20	Khulgunskaya	LP	P	Bolotnikova (1977)
16	Urkan, Amur Region, Russia	54°10'	124°39'	IRC	21	Kivdinskaya	LP	P	Sorokin and Belousov (1984)
17	Snezhnegorskoe, Amur Region, Russia	54°10'	127°60'	IRC	22	Raichikhinskaya	EE	P	Kezina and Ol'kin (2000)
18	Pikanskii, Amur Region, Russia	53°50'	127°10'	IRC	23	Verkhnetsagayanskaya	EP	P	Kezina (1997, 2005)
19	Tygda245, Amur Region, Russia	53°06'	126°20'	IRC	24	Verkhnetsagayanskaya	EP	P	Kezina (2005)
20	Ushumunskii5, Amur Region, Russia	52°50'	126°30'	IRC, SC	25	Raichikhinskaya	EE	P	Varnavskii et al. (1988)
				IRC, SC	26	Kivdinskaya	LP	P	Varnavskii et al. (1988)
21	Malomikhailovka, Khabarovsk Region, Russia	52°00'	140°00'	IRC	27	Malomikhailivskaya	EP	P, L	Akhmetiev (1973, 1993), Akhmetiev and Golovneva (1998), Akhmetiev et al. (2009), Pavlyutkin and Petrenko (2010)
22	Bukhta Siziman, Khabarovsk Region, Russia	50°40'	140°30'	IRC	28	Kizinskaya	EE	L	Ablaev et al. (2005), Akhmetiev (1973, 1988), Pavlyutkin and Petrenko (2010)
23	Erkovtsy, Amur Region, Russia	50°36'	128°30'	IRC, SC	29	Raichikhinskaya	EE	P, L	Baikovskaya (1950), Brattseva (1969), Kezina (2005)
				IRC, SC	30	Kivdinskaya	LP	P, L	Kamaeva (1990), Kezina (2005), Mamontova (1977), Naryshkina (1973), Ziva (1973)
				IRC, SC	31	Verkhnetsagayanskaya	EP	P, L	Kezina (2005), Kezina and Litvinenko (2007), Ziva (1973)
24	Darmakan, Amur Region, Russia	49°60'	129°60'	IRC	32	Verkhnetsagayanskaya	EP	L	Krassilov (1976), Zaklinskaya et al. (1977)
25	Raichikhinsk, Amur Region, Russia	49°50'	129°20'	IRC, SC	33	Raichikhinskaya	EE	P, L	Fedotov (1983), Kezina (2005)
				IRC, SC	34	Kivdinskaya	LP	P	Kezina (2005), Ziva (1973)
26	Avgustovka, Sakhalin Island, Russia	49°40	142,10	IRC	35	Kamenskaya (Podkonglomeratnye sloi)	EP	P, L	Ablaev (1976), Gladenkov et al. (2002), Kodrul (1999), Zaklinskaya (1976)
27	Svobodnoe53, Amur Region, Russia	49°30'	129°30'	IRC, SC	36	Raichikhinskaya	EE	P	Kezina (2005)
				IRC, SC	37	Kivdinskaya	LP	P	Kezina (2005)
				IRC, SC	38	Verkhnetsagayanskaya	EP	P	Kezina (2005)
28	Snezhinka, Sakhalin Island, Russia	49°20'	142°15'	IRC, SC	39	Snezhinkinskaya (upper subformation)	EE	P, L	Gladenkov et al. (2002), Kodrul (1999)
				IRC, SC	40	Snezhinkinskaya (middle subformation)	LP	L	Gladenkov et al. (2002), Kodrul (1999)
				IRC, SC	41	Snezhinkinskaya (lower subformation)	EP	P, L	Gladenkov et al. (2002), Kalishevich et al. (1981), Kodrul (1999)
29	Snezhinka, Sakhalin Island, Russia	49°20'	142°10'	IRC	42	Boshnyakovskaya (Kamskie sloi)	EP	P	Gladenkov et al. (2002), Kalishevich et al. (1981)
30	Kama, Sakhalin Island, Russia	49°20'	142°06'	IRC	43	Boshnyakovskaya (Kamskie sloi)	EP	L	Akhmetiev et al. (1978), Gladenkov et al. (2002), Kodrul (1999), Sycheva (1975)
31	Arkharo-Boguchan, Amur Region, Russia	49°18'	130°12'	IRC	44	Verkhnetsagayanskaya	LP	L	Moiseeva et al. (2018)

Table 1. (continued)

Site	Location	Coordinate		Age control	PA	Formation/group (member)	Age	Fossil type	References
		Lat	Lon						
32	Baishantou, Heilongjiang Province, China	49°14'	129°28'	IRC	45	Wuyun	EP	P, L	Chen et al. (2004), Hao et al. (2010), Kezina (2005), Manchester et al. (1999), Muling (1983), Tao and Xiong (1986)
33	Shakhtnyi, Sakhalin Island, Russia	48°30'	142°40'	IRC	46	Krasnoyarkovskaya (Sinegorskie sloi)	EP	P	Gladenkov et al. (2002), Zaklinskaya (1976)
34	Birofel'd, Jewish Autonomous Region, Russia	48°20'	132°50'	IRC	47	Cernorechenskaya (lower subformation)	EE	P	Pavlyutkin and Petrenko (2010), Ziva and Lukashova (1977)
35	Naiba, Sakhalin Island, Russia	47°50'	142°30'	IRC	48	Boshnyakovskaya (Kamskie sloi)	EP	P	Gladenkov et al. (2002), Zaklinskaya (1976)
36	Ozero Toni, Primorye Region, Russia	47°40'	138°30'	IRC	49	Kizinskaya	EE	P, L	Oleinikov and Klimova (1977), Varnavskii et al. (1988)
37	Krasnoyarka, Sakhalin Island, Russia	47°40'	142,50	IRC, SC	50	Naibutinskaya (upper levels)	EE	P, L	Gladenkov et al. (2002), Kodrul (1999)
				IRC, SC	51	Naibutinskaya (lower levels)	LP	L	Gladenkov et al. (2002), Kodrul (1999)
38	Alchan, Primorye Region, Russia	46°87'	134°94'	IRC	52	Uglovskaya	EE	P	Pavlyutkin and Petrenko (2010), Krasnyi (1994)
39	Bikin, Primorye Region, Russia	46°57'	135°09'	IRC	53	Unamed unite	EE	P	Pavlyutkin and Petrenko (2010), Krasnyi (1994)
40	Luchegorsk540/541, Primorye Region, Russia	46°30'	134°20'	IRC	54	Unamed unite	EE	P, L	Pavlyutkin and Petrenko (2010)
41	Kril'on,Sakhalin Island, Russia	46°30'	142°10'	IRC, SC	55	Snezhinkinskaya (upper subformation)	EE	P	Fotjanova et al. (2001), Gladenkov et al. (2002)
				IRC, SC	56	Krasnoyarkovskaya (Sinegorskie sloi)	EP	P	Fotjanova et al. (2001), Gladenkov et al. (2002)
42	Kluch Kedrovyi, Primorye Region, Russia	46°17'	137°78'	IRC	57	Kedrovskaya	LP	P	Varnavskii et al. (1988)
43	Yilan, Heilongjiang Province, China	46°10'	129°30'	GD	58	Xin'ancun	EE	P	Quan et al. (2012a, b)
44	Kluch Stolbikova, Primorye Region, Russia	46°05'	137°50'	GD	59	Kuznetsovskaya	LP	L	Pavlyutkin and Petrenko (2010), Varnavskii et al. (1988)
45	Sobolevka, Primorye Region, Russia	46°05'	137°50'	GD	60	Takhobinskaya	EP	L	Akhmetiev (1973, 1988), Borsuk (1952)
46	Krylovskii524, Primorye Region, Russia	45°10'	133°40'	IRC	61	Uglovskaya	EE	P	Pavlyutkin and Petrenko (2010)
47	Hualin, Heilongjiang Province, China	44°80'	129°80'	PD, SC	62	Bahuli	EE	P	Quan et al. (2012a, b)
48	Shulan, Jilin Province, China	44°50'	126°90'	M, PD	63	Bangchuigou	EE	P	Fan (1985), Quan et al. (2012a)
49	Rettikhovka, Primorye Region, Russia	44°10'	132°40'	IRC	64	analog of Uglovskaya	EE	P	Pavlyutkin and Petrenko (2010)
50	Arsen'evka, Primorye Region, Russia	44°10'	133°10'	IRC	65	analog of Uglovskaya	EE	P	Bolotnikova (1988)
51	Kluch Tuyanov, Primorye Region, Russia	44°10'	135°10'	IRC	66	Tujanovskaya	EE	L	Baskakova and Lepekhina (1990), Varnavskii et al. (1988)
52	Ustinovka, Primorye Region, Russia	44°10'	135°10'	IRC, SC	67	Tadushinskaya	LP	L	Pavlyutkin and Petrenko (2010)
				IRC, SC	68	Bogopol'skaya	EP	L	Ablaev et al. (2005), Krassilov (1989)
53	Tavrichanka9142, Primorye Region, Russia	43°30'	131°50'	M	69	Uglovskaya analog of	EE	P	Pavlyutkin and Petrenko (2010)

Table 1. (continued)

Site	Location	Coordinate		Age control	PA	Formation/group (member)	Age	Fossil type	References
		Lat	Lon						
54	Smolyaninovo, Primorye Region, Russia	43°20'	132°30'	IRC	70	Uglovskaya	EE	P, L	Baskakova and Gromova (1979, 1984), Pavlyutkin and Petrenko (2010), Tashchi et al. (1996), Varnavskii et al. (1988), Verkhovskaya and Kundyshev (1989)
55	Kluch Ugolnyi, Primorye Region, Russia	43°20'	134°10'	IRC	71	Uglovskaya	EE	P, L	Chekryzhov et al. (2010), Pavlyutkin and Petrenko (2010)
56	Fushun, Liaoning Province, China	41°80'	123°90'	GD, PD	72	Guchengzi	EE	P	Hong et al. (1980), Quan et al. (2012a)
57	Fushun, Liaoning Province, China	41°50'	123°54'	IRC	73	Guchengzi	EE	P	Wang et al. (2010)
				IRC	74	Lizigou	LP	P	Hong et al. (1980), Wang et al. (2010)
				GD, PD	75	Laohutai	EP	P	Hong et al. (1980), Wang and Wang (1982, 1985), Wang et al. (1982, 2010)
58	Etuoke, Inner Mongolia, China	39°10'	107°90'	M	76	Unamed unite 1 (lower)	EE	P	Song and Zhang (1990), Quan et al. (2012a)
59	Shache, Xinjiang Province, China	38°30'	77°30'	CN, Fo	77	Kalataer	EE	P	Wang et al. (1986), Quan et al. (2012a)
60	Huanghua, Hebei Province, China	38°30'	117°30'	GD, PD	78	Shahejie (part IV)	EE	P	Zhang and Yin (2005), Quan et al. (2012a)
61	Changle, Shandong Province, China	36°70'	118°80'	G, V	79	Wutu	EE	P	Wang (2005), Quan et al. (2012a)
62	Xining, Qinghai Province, China	36°50'	101°70'	O, PD	80	Qijiachuan (parts III, IV)	EE	P	Sun et al. (1980), Quan et al. (2012a)
63	Wutu, Shandong Province, China	36°39'	118°55'	M	81	Wutu	EE	P	Zhang et al. (2016), Quan et al. (2012a)
64	Lanzhou, Gansu Province, China	36°10'	103°80'	PD	82	Unamed unite 2 (lower)	EE	P	Ma et al. (1995), Quan et al. (2012a)
65	AS_Japan, Japan	36°00'	138°00'	IRC	83	Unamed unite	EE	L	Tanai (1972)
66	Luanchuan, Henan Province, China	33°80'	116°60'	M, R	84	Tantou (lower)	EE	P	Wang et al. (1984), Quan et al. (2012a)
67	Gaoyou, Jiangsu Province, China	32°80'	119°40'	O	85	Dianan	EE	P	Zhang and Qian (1992), Quan et al. (2012a)
68	Hefei, Anhui Province, China	31°86'	117°28'	C, D	86	Dingyuan (part III)	EE	P	Wang et al. (1987), Quan et al. (2012a)
69	Jianghau, Hubei Province, China	30°40'	112°80'	O	87	Xingouzui	EE	P	Wang and Zhao (1980), Quan et al. (2012a)
70	Qingjiang, Jiangxi Province, China	27°90'	116°10'	C, M, O	88	Qingjiang (part I)	EE	P	He and Sun (1977), Quan et al. (2012a)
71	Donghai, Zhejiang Province, China	26°40'	121°70'	Fo, CN	89	Oujiang	EE	P	Zhang et al. (1990), Quan et al. (2012a)
72	Zhujiang, Guangdong Province, China	22°60'	113°30'	GD, MA	90	Lufeng	EE	P	Li (1998), Quan et al. (2012a)
73	Changchang, ? China	19°38'	110°27'	IRC	91	Changchang	EE	P	Yao et al. (2009)

References and complete flora lists including Nearest Living Relatives used for vegetation analysis are given in Appendix 1. Sites are shown in Fig. 3. Age control in addition to plant assemblages (PA): IRC – inter-regional correlation; C – charophyte; CN – calcareous nannofossils; D – dinoflagellate; Fo – foraminifera; G – gastropods; GD – geochemical dating; M – mammals; MA – marine animals; Mo – mollusks; O – ostracods; PD – paleomagnetic dating; SC – stratigraphical correlation; R – reptiles; V – vertebrates. Age: EE – early Eocene; LP – late Paleocene; EP – early Paleocene. Fossil type: L – leaf; P – pollen and spores; C – seeds and fruits.

regarding the validity of taxonomic identifications and Nearest Living Relatives (NLRs) of the fossil taxa. We analysed a total of 110 floras including 79 palynofloras (PF), 30 leaf floras (LF) and one carpoflora (CF) with respect to palaeoclimate considering three time slices, namely the early Palaeocene, late Palaeocene, and early Eocene.

The assignment of the palaeofloras to the three time slices considered here is done on the basis of stratigraphic information available in literature and compiled in Table 1. In many cases, flora-bearing horizons originate from longer successions that are tied to regional stratigraphy and partly cover the early Palaeocene to early Eocene (e.g. Kolyma1, Slezovka15, Erkovtsy, etc.) thus facilitating a consistent sample selection. The single floras are listed in ESM 1, together with information on basin provenance, type of flora, stratigraphic age, method of dating, and references. The complete floral lists, assigned NLRs and their climatic requirements are given in ESM 1. For the early Palaeocene, a total of 25 floras is available, all within a relatively narrow latitudinal range from 41.50 to 67.06° N (Fig. 3c and f). For the late Palaeocene, the compilation comprises 21 floras within the range from 41.50 to 71.50° N (Fig. 3b and e). The early Eocene record includes 64 floras covering the widest latitudinal range, from 19.38 to 75.53° N (Fig. 3a and d).

Application of the Coexistence Approach (CA)

To reconstruct quantitative precipitation data from the plant fossil record we use the CA (Mosbrugger and Utescher 1997; Utescher et al. 2014). This approach is organ-independent, so that both macro- and microfossil floras can be used as long as their modern botanical affinities are determinable (Mosbrugger and Utescher 1997; Utescher et al., 2007; Bruch et al. 2011). We use data sets from the Palaeoflora Database (Utescher and Mosbrugger 2018) as source for climatic requirements of extant plant taxa. New climate requirements of plants were compiled using chorological information from Fang et al. (2009, 2011) and Sokolov et al. (1977, 1980, 1986), and climatological data from Müller and Hennings (2000) and New et al. (2002). Climate data entries already available in the database were carefully checked for completeness. Floral lists with corresponding NLRs employed in this study and their climatic requirements are made available in ESM 1.

In this study, four precipitation variables are reconstructed: mean annual precipitation (MAP), mean precipitation of dry, wet and warm months (MPdry, MPwet and MPwarm). In the CA, at least 10 NLR taxa contributing with climate data are required to obtain reliable results (Mosbrugger and Utescher 1997). Here, 9 to 82 (mean 33.3) taxa contribute to determining the coexistence intervals – CIs (ESM 2). The climatic resolution of the CA results also depends on the taxonomical level of the NLR assignment (Mosbrugger and Utescher 1997). For the Paleogene floras, we use genera or family levels for NLRs. For monotypic genera (but not monotypic families) we use climate data for (sub)families. Moreover, ca. 50 (sub)-cosmopolitan taxa were not considered in CA analysis. For a total of ca. 10 taxa climatic tolerances are not reliably known. *Eucommia ulmoides* Oliver, *Ginkgo biloba* L. and *Sciadopitys verticillata* (Thunb.) Siebold et Zucc. were excluded from the analysis for being monotypic taxa (cf. Bondarenko and Utescher 2022).

The distribution of modern Koeppen–Geiger type climates of Eurasia, modern MAP and ratios of MPwet to MAP (RMPwet) over Eurasia are given in Figure 1. To illustrate temperature gradients along the Pacific side of Eurasia during the early Paleogene, the floras are allocated to three time intervals. These time intervals are defined according to the international standard: early and late Palaeocene, and early Eocene. To visualize the results, a series of palaeogeographic maps is provided and discussed below. The maps, which trace the evolution of the three precipitation variables (MAP, MPdry and MPwet) throughout the early Paleogene, are based on means of coexistence intervals for each palaeoflora and averaged for the time intervals considered (Fig. 3 and 4). The differentiation of climatic zones is based on a significant change in the prevailing mean values of MAP. The complete set of coexistence intervals for all floras and climate variables studied is provided in ESM 2. For the technical preparation of the maps, ArcMAP 10.4 was used. We use rotated coordinates (using ODSN Plate Reconstruction Service for 55 Ma and hotspot reference frame I) for the palaeosites showing zonal means (Figs. 3–8).

In order to determine precipitation seasonality of the early Paleogene climate of the Pacific side of Eurasia, the mean annual range of precipitation (MARP) was calculated as the difference of MPwet and MPdry for the time intervals studied (Fig. 5; ESM 2). In order to obtain a measure of monsoon intensity during the early Paleogene we use the ratios of MPwet and MPdry to MAP (RMPwet and RMPdry) (Fig. 6; ESM 2).

Results

A complete list of taxa for each of the localities, including their NLRs with precipitation requirements, is provided in ESM 1. Precipitation data calculated for the 110 floras are given in ESM 2. CA-based precipitation data are obtained from a total of 79 microfloras (mean diversity of taxa contributing with climate data: 37, std. 14) and 30 macrofloras (mean diversity of taxa contributing with climate data: 25, std. 13) largely providing reliable results (>10 taxa; cf. Mosbrugger and Utescher 1997), except for the early Palaeocene LF 7, early Eocene PF 38 and LF 23. In the calculations of all considered variables the proportion of coexisting NLR taxa exceeds 98 %. This indicates a high

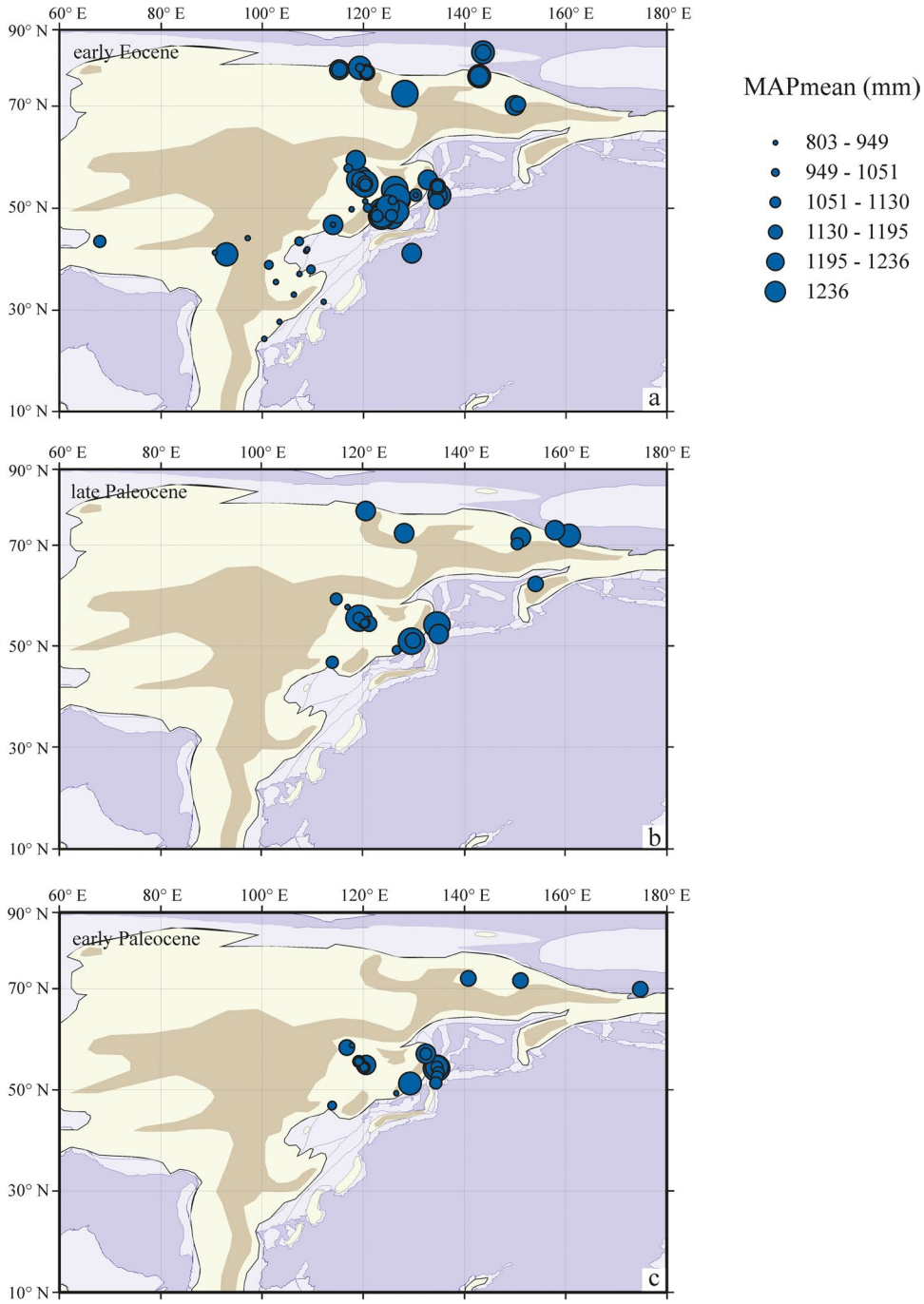

Fig. 3. Spatial MAP distributions along the Pacific side of Eurasia during the early Paleogene

significance level of the results (Mosbrugger and Utescher 1997) and the integrity of the applied NLR concept that mainly employs families and genera, but in single cases also refers to the species level. Occasionally, multiple CIs at a close climatic range are obtained, most probably related to integration over several flora-bearing horizons and/or taphonomic effects (Utescher et al. 2014). The application of a NLR concept at high taxonomic levels, as is necessary with early Palaeogene records, inevitably results in a moderate precision of the obtained CIs. Using the example of MAP, the mean precision, i.e. the mean width of the CIs for all floras amounts to 605 mm (std. 333.6 mm).

CA results for 18 floristic levels containing both micro- and macrofloras are largely congruent. However, it is shown that overall narrower precipitation ranges are obtained from the mainly local and taxonomically better-resolved macrofloras. The CIs reconstructed for the macrofloras tend to cover the drier ends of the broader ranges derived in the coeval microflora-based reconstruction having a lower climatic resolution and reflecting regional rather than local climate.

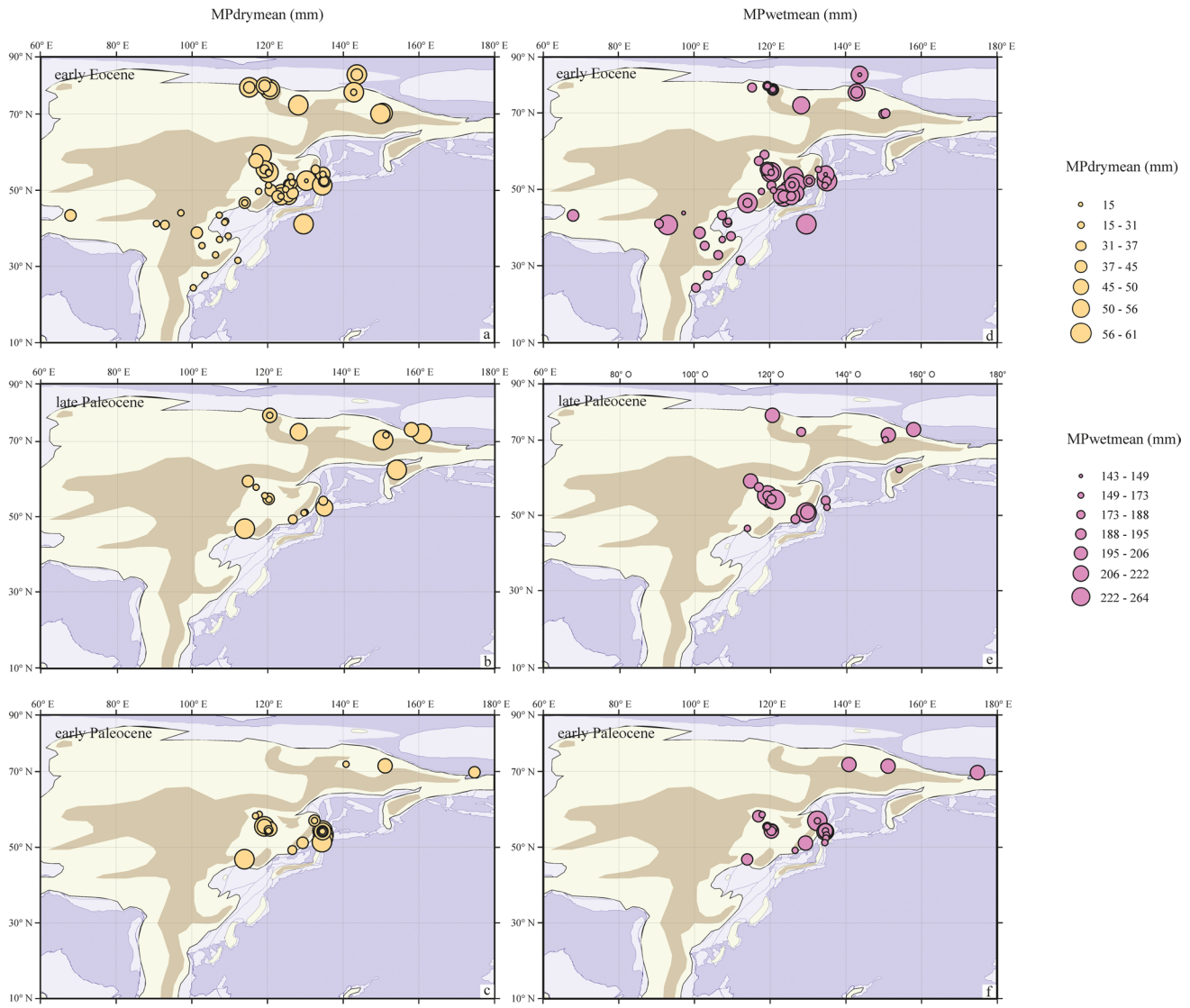

Fig. 4. Spatial distributions of MPdry and MPwet along the Pacific side of Eurasia during the early Paleogene

Based on means of coexistence intervals obtained for each palaeoflora, a high humidity level regarding MAP, MPdry and MPwet is observed for the early Paleogene. A minor increase of the mean annual range of precipitation (MARP) from the early Palaeocene (mean 131 mm; std 32) to the late Palaeocene (mean 140 mm; std 36) and early Eocene (mean 137 mm; std 30) may indicate a trend to more seasonal climates. Based on MAP (Fig. 3a-c), MPdry (Fig. 4a-c) and MPwet (Fig. 4d-f) data, our results suggest the existence of two different regional precipitation regimes to the north and south of ca. 50° N palaeolatitude persisting throughout all time slices regarded.

In the northern part, typical MAP CIs range from 979–1355 mm and 1090–1355 mm, with the lower CI limits defined by *Corylopsis* Siebold et Zucc. and *Altingia* Noronha, respectively. In the southern part, taxa indicative for high MAP >900 mm were absent from most floras while typical CIs of 652–1096 mm or 740–1096 mm are delimited by *Podocarpus* L'Heritier ex Persoon/Engelhardioideae Iljinsk. and *Ephedra* L. towards wet conditions. Between both zones, within the range of ca. 45° and 55° N palaeolatitude, a transition zone can be distinguished where floras yielding higher and lower values of all precipitation parameters coexisted, indicating shorter-term boundary shifts that are temporally unresolvable by our time slice concept. In the northern part, typical MPwet CIs range from 178–196 mm and 180–245 mm, with the lower CI limits defined by *Reevesia* Lindl. and *Altingia*, respectively. In the southern part, taxa indicative for high MPwet >150 mm were absent from most floras while typical CIs of 150–220 mm are delimited again by Engelhardioideae and *Ephedra*. In the northern

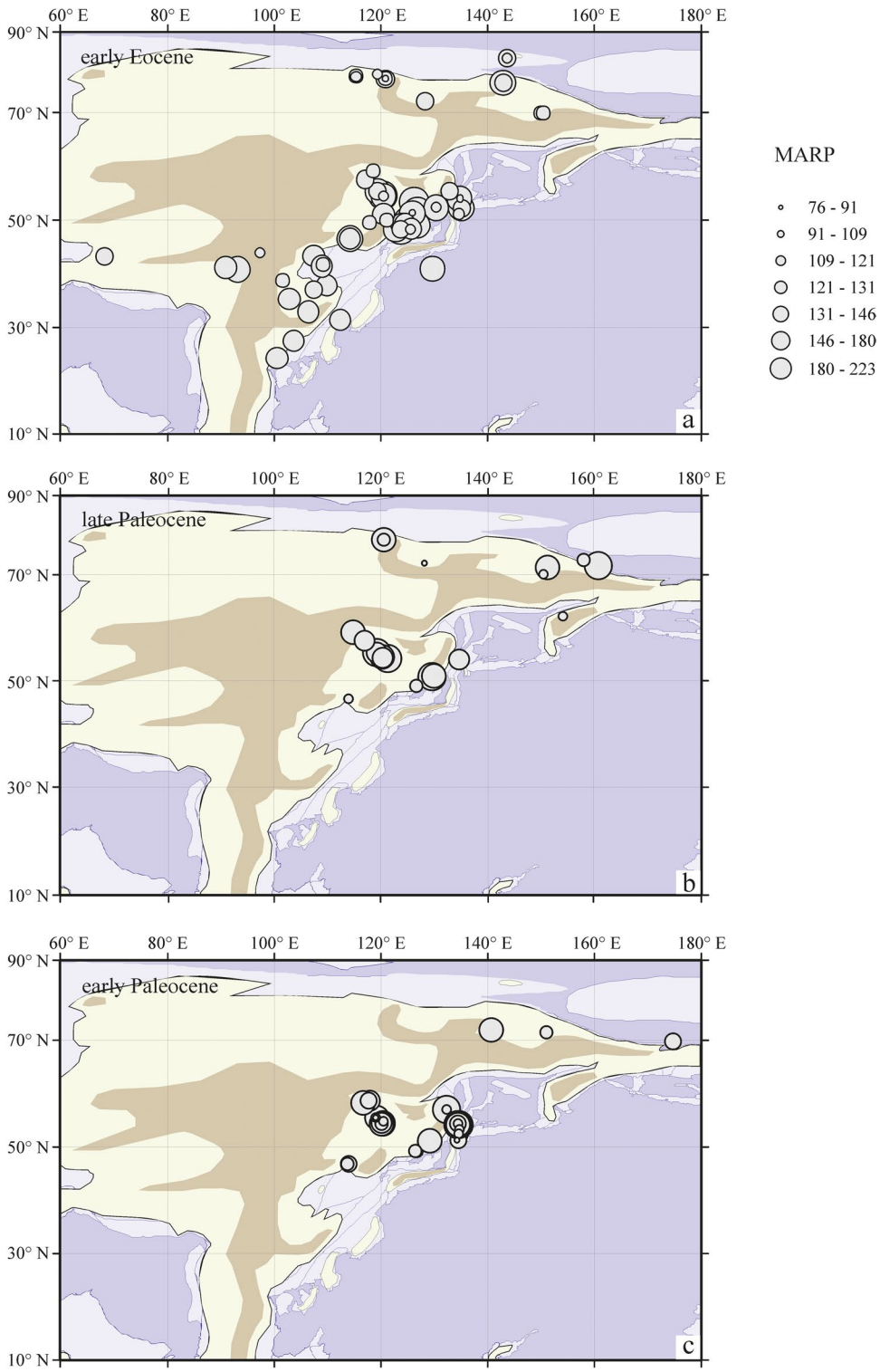

Fig. 5. Spatial distributions of MARP along the Pacific side of Eurasia during the early Paleogene

part, typical MPdry CIs range from 42–67 mm and 50–80 mm, with the lower CI limits defined by *Fothergilla* Murr. and *Planera* Gmelin, respectively. In the southern part, taxa indicative for high MPdry >13-17 mm were absent from most floras while typical CIs of 17–45 mm are delimited again by *Podocarpus* and *Ephedra*.

The spatial patterns of mean values of RMPdry (Fig. 6a-c) and RMPwet (Fig. 6d-f) are similar to the patterns for MAP, MPwet and MPdry, and demonstrate the existence of two different regional precipitation regimes to the north and south of ca. 50° N palaeolatitude. In the northern part, RMPwet is in range from 12.5 to 18.1 %, while in the southern part – from

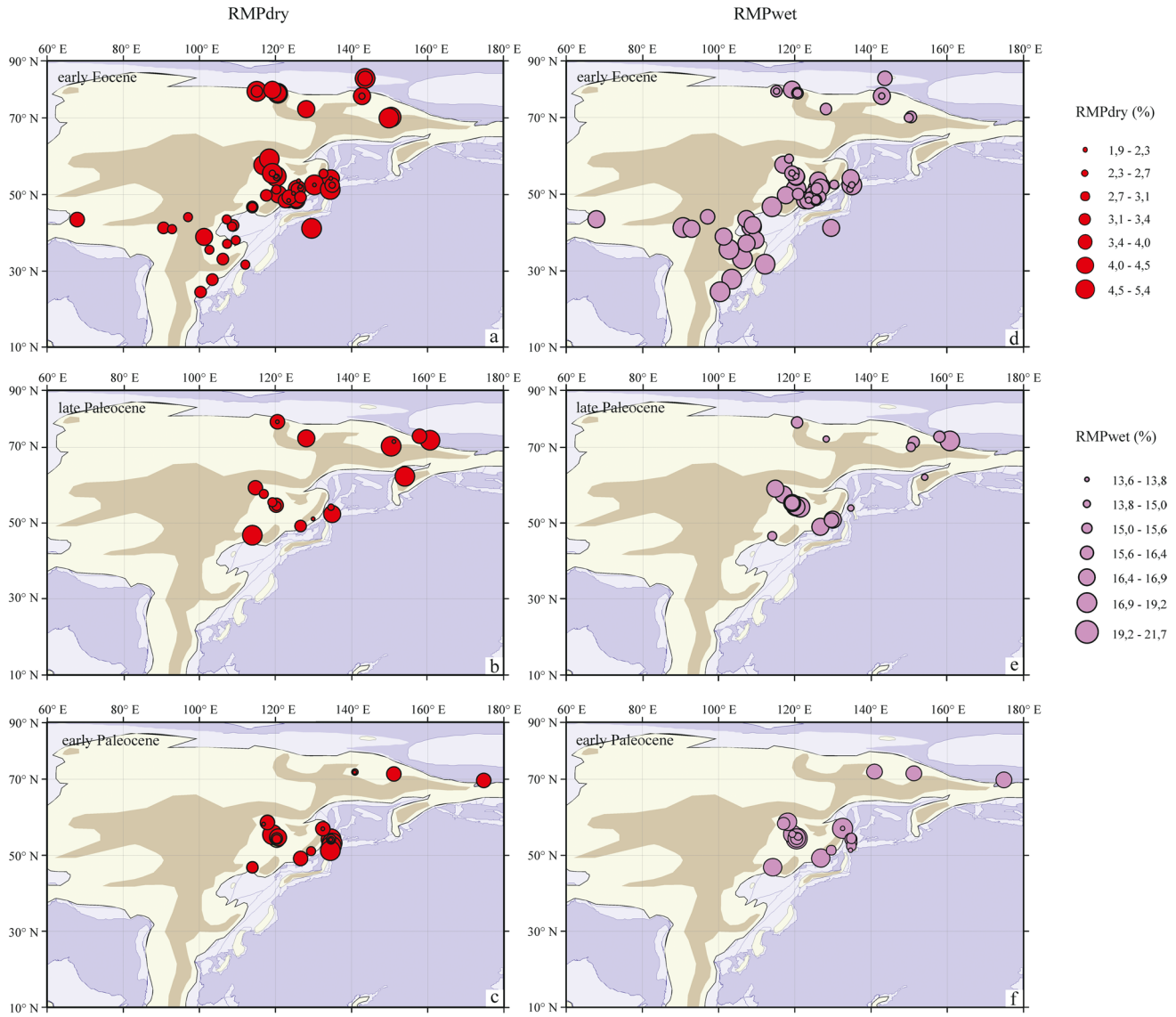

Fig. 6. Spatial distributions of RMPdry and RMPwet along the Pacific side of Eurasia during the early Paleogene

13.3 to 24.1 %. In the northern part, RMPdry is in range from 2.5 to 5.1 %, while in the southern part – from 2.9 to 4.8 %.

Discussion

Early Paleogene precipitation in Eurasia and comparison with other proxy-based precipitation reconstructions and zonal gradients

Palaeocene

According to Bondarenko and Utescher (2022), the latitudinal temperature gradient was very weak during the early Paleogene. Likewise, the early Palaeocene precipitation gradients were very weak. Based on means of MAP data, our palaeoprecipitation reconstruction reveals more equable humid conditions for the studied region compared to the other time slices considered. Unfortunately, the available sites only provide data for the latitudinal sector north of ca. 48° N so that conditions at lower latitudes cannot be assessed. A minor gradient is observed between the southern and northern sectors, with MAPmean mostly being as high as ca. 1100–1200 mm at 70° N, and ca. 1000–1100 mm at 50° N, except for Sakhalin – 1300–1600 mm (Fig. 3c). These results are in general agreement with the CLAMP-based reconstruction by Akhmetiev (2004) revealing two climatic zones in the Northern Hemisphere

during the Palaeocene, namely a (warm) temperate humid zone, and a humid subtropical and paratropical zone. According to Akhmetiev (2004), the southern boundary of the first zone of temperate warm climate at the beginning of the Palaeocene was near 59° N (Akhmetiev 2004). Based on CLAMP analysis, Akhmetiev (2004) suggested a MAP of up to 1400 mm for the northerly zone, and MAP rates of 1500–2000 mm for southerly zone. These values do not overlap with the actual CA-based reconstruction. Our precipitation data are lower in general and show a reverse gradient.

However, our values are similar to precipitation level and spatial gradient reconstructed by Budantsev (1999) based on CLAMP. According to Budantsev (1999), in the south of the RFE (Sakhalin and Primorye) MAP reached 1168 mm, while in the north (Koryak Upland) MAP was 1377 mm. Using CA, Bondarenko et al. (2020b) estimate MAP across the early Palaeocene in the Amur Region ranging between 1100–1600 mm. For the early Palaeocene of Primorye, Bondarenko et al. (2020a) reconstructed MAP ca. 1000–1300 mm. For the early Palaeocene of northeastern China, Quan et al. (2012b) indicated MAP in range from 815 to 1389 mm.

For the Late Cretaceous and early Paleogene in the mid-latitude Northern Hemisphere (e.g. East Asia), Chen et al. (2022) suggest that the past MAP patterns were correlated with warming and cooling phases. The warm phases (e.g. at ~69.5–68.5 Ma) were characterised by increased MAP, related to the the higher temperature contrast between the ocean and land, while in the periods of global cooling (e.g. at ~72.5–69.5 Ma and ~68.5–66.5 Ma), MAP decreased due to a weakened EAM and intensified equatorward-shifted Westerlies.

The late Palaeocene precipitation pattern in our reconstruction does not show any substantial changes compared to the early Palaeocene (Fig. 3b). In the late Palaeocene, a minor MAP gradient from mid- to high latitudes also can be observed: ca. 1100–1200 mm at 70° N, and ca. 1000–1100 mm at 50° N, except for Sakhalin – 1300 mm. However, the available sites (the same as for the early Palaeocene) only provide data for the latitudinal sector N of ca. 48° N so that conditions at lower latitudes cannot be assessed.

The high precipitation indicated for the Canadian Arctic in the Palaeocene (Greenwood et al. 2010) was perhaps characteristic of the Arctic during the early Paleogene (e.g. Uhl et al. 2007; Eldrett et al. 2009). According to Budantsev (1999), MAP reached 1300 mm in the coastal regions of the northeast of Asia (55–60° N) during the late Palaeocene and in the continental regions (north of Yakutia) up to 1200 mm, in the south of the RFE (Sakhalin, Primorye), a MAP of 826 mm is reconstructed. Using the CA method, Bondarenko et al. (2020b) inferred overall humid climate conditions with MAP 1278–1740 mm throughout the late Palaeocene in the Amur Region (RFE). Bondarenko et al. (2020a) recognised MAP values of 1045–1210 mm for the late Palaeocene in Primorye. For the late Palaeocene of northeastern China, Quan et al. (2011, 2012b) indicated a range of MAP from 897 to 1355 mm.

Early Eocene

In the early Eocene, the MAP gradient became more clearly pronounced, and a larger "arid" zone can be distinguished in the mid-latitudes. The early Eocene MAP gradients are basically NW-SE oriented. Spanning a latitudinal range of ca. 20° N to the High Arctic, early Eocene data most comprehensively reflect the latitudinal precipitation pattern in the Paleogene of Pacific Eurasia. For the High Arctic, CA interval means indicate wet conditions in the order of 1200–1300 mm for MAP (Fig. 3a). These data are close to CLAMP-based precipitation estimates for early Eocene floras of northern Yakutia and the Far East (MAP ca. 1200 mm, cf. Budantsev 1999). While the mid-latitudinal precipitation did not differ significantly from the earlier time slices studied, the lower precipitation level obtained from the lower latitude sites located south of 45° N is noteworthy, with MAP not exceeding ca. 1100 mm. For the early Eocene of northeastern China, Quan et al. (2012b) reconstructed MAP ranges from 373 to 1577 mm, with more specific ranges of 1000−1100 mm. For the early Eocene of China, Quan et al. (2012a) gave MAP values ranging from 735 to 1632 mm, with more specific ranges of 1100–1200 mm. Recent studies on middle and late Eocene floras of south China revealed humid subtropical conditions, with CLAMP-based estimates being in the order of the presently reconstructed early Eocene data (GSP 200−240 mm; cf. Jin et al. 2017).

Based on CLAMP data, Wolfe (1994, 1995) suggested generally high MAP from 1000 to 2000 mm for the Eocene of Pacific North America and thus proposed conditions that are comparable to our East Asian Pacific data. For the early Eocene climate of northern part of North America, warm and wet conditions are suggested, with MAT (mean annual temperare) ~20 °C and MAP at 1000–1500 mm (Wing and Greenwood 1993; Wing 1998; Shellito and Sloan 2006; Smith et al. 2012; Breedlovestrout et al. 2013; Herold et al. 2014; Greenwood et al. 2016; West et al. 2020). For the early Eocene floras from the London Clay, UK, MAP was determined as more than 2000 mm (Van Beuskom 1971).

As regards the lower latitudes of the Atlantic realm during the early Eocene published records provided overall wetter conditions, compared to our Pacific record. In the southeast of North America, the floras are already predominantly tropical type (Akhmetiev 2004). Climatic characteristics, calculated by Greenwood and Wing (1995) using the CLAMP method for the early Eocene or early – middle

Eocene floras of the Canadian Arctic Archipelago (79°55' N), is MAP 1000−2000 mm.

Earlier, East Asian Paleogene climates were subdivided into three latitudinal zones, which are, at least partly, defined by hydrological constraints (e.g. Liu 1997; Wang et al. 1999; Akhmetiev 2004; Guo et al. 2008; Z. Zhang et al. 2012) that partly are reflected in the temperature reconstructions (Bondarenko and Utescher 2022). Two humid zones were located in the south and north, while the third broad arid zone occurred in the middle and flanked by the two humid zones along ca. 30° N palaeolatitude (ranging between ~25° N and ~35° N), allegedly driven by the then subtropical highs (Liu 1997; Wang et al. 1999; Guo et al. 2008; Z. Zhang et al. 2012). In our reconstruction of precipitation, only provisionally can two subzones be distinguished: wetter (to the north of 50° N palaeolatitude) and drier (to the south of 50° N palaeolatitude).

Generally, our data show a higher level of MAP, MPdry and MPwet for the high and higher mid-latitudes of the Pacific areas of Eurasia in the early Paleogene compared to the present-day. This correlates well with higher MAT, cold month mean temperature (CMMT), and warm month mean temperature (WMMT) values, as well as with a latitudinal temperature gradient on the Pacific side of Eurasia in the early Eocene, being about only one third of the present (e.g. Wolfe 1978; Greenwood and Wing 1995) or even less, as suggested by the Pacific data (Bondarenko and Utescher 2022). Higher temperatures lead to higher evaporation of water, resulting in higher levels of precipitation.

Precipitation patterns – correlation with global atmospheric circulation

Global atmospheric circulation as a large-scale movement of air leads to the transfer of matter and energy in both latitudinal and meridional directions, which is the most important climate-forming process. The circulation of the atmosphere varies from year to year and leads to the formation of cyclones, anticyclones, monsoons and trade winds. At the same time, the global structure of atmospheric circulation fundamentally remains constant and determines the existence of latitudinal zonality (Pogosyan 1972). Today the wind belts girdling the planet are organised into three cells in each hemisphere – the Hadley cell in the tropics, the Ferrel cell in the mid-latitudes, and the polar cell at high latitude regions (Huang and McElroy 2014; Fig. 7a).

As mentioned above, our reconstructions of palaeoprecipitation for the Pacific side of Eurasia in the early Paleogene demonstrate a clear division (especially pronounced in the early Eocene) into two zones at ca. 50° N palaeolatitude on all precipitation parameters – MAP (Fig. 3a-c), MPdry (Fig. 4a-c) and MPwet (Fig. 4d-f). Between both zones, within the range of ca. 5° to south and north from 50° N palaeolatitude, a transition zone can be distinguished where the presence of higher and lower values of all precipitation parameters is observed. By the way, similar patterns are also observed for temperature parameters (Bondarenko and Utescher 2022). Thus, our data suggest that in the early Paleogene, the global atmospheric circulation consisted of two well-defined cells, Hadley and Ferrell, while the polar cell was either absent or located over the Arctic Ocean and was very weak. This explains the presence of a drier zone to the south and a wetter zone to the north. It seems that the boundary between the Hadley and Farrell cells ran at about 50° N palaeolatitude, while the transition zone can reflect the possible shorter-term migration/shifting area of these cells (Fig. 7b-d). The asymmetric (NW-SE) orientation of these two zones is mirrored the northward energy transport by ocean and atmosphere. Comparable conditions of a very humid and warm Arctic may have existed during the early Late Cretaceous (Spicer et al. 2019). According to Spicer et al. (2019), it is likely that at that time the polar front was more diffuse and displaced towards the pole in comparision to present, while a warm Arctic Ocean is considered a key component of a then weaker polar high.

Precipitation seasonality

The modern climate of eastern Eurasia in high and mid latitudes is characterised by pronounced temperature and precipitation seasonality. At the same time, the seasonal contrast of temperature today increases to the north and even more to the northeast, and precipitation contrast, to the contrary, decreases to the north. The modern spatial pattern of RMPwet over Eurasia, as an illustration of precipitation seasonality, is shown in Figure 1c.

As mentioned above, all our precipitation data suggest the pronounced precipitation seasonality of the early Paleogene climate over East Asia. The higher past MPwet coupled with distinctly higher MPdry indicate that, during the early Paleogene, the climate of Eastern Eurasia in general was more humid. In turn, this is in good agreement with the high level of MAP. It is interesting to note that under the existence of two zones, a wetter (north of 50° N palaeolatitude) and a drier (south of 50° N palaeolatitude), MARP values are similar across the studied sector, i.e. show no significant gradient nor any zonal arrangement (Fig. 5a-c). Moreover, all localities are characterised by a marked difference in the MPwet/MPdry ratio, which mainly varies from 3:1 to 8:1, but for some macrofloras even from 10:1 to 15:1 (ESM 2). Such a large range can most likely be explained by topography, distance from the sea/ocean, and local conditions.

A pronounced seasonality of precipitation was suggested by many researchers for the late Cretaceous and early Cenozoic. Spicer et al. (2019) estimate a marked difference in

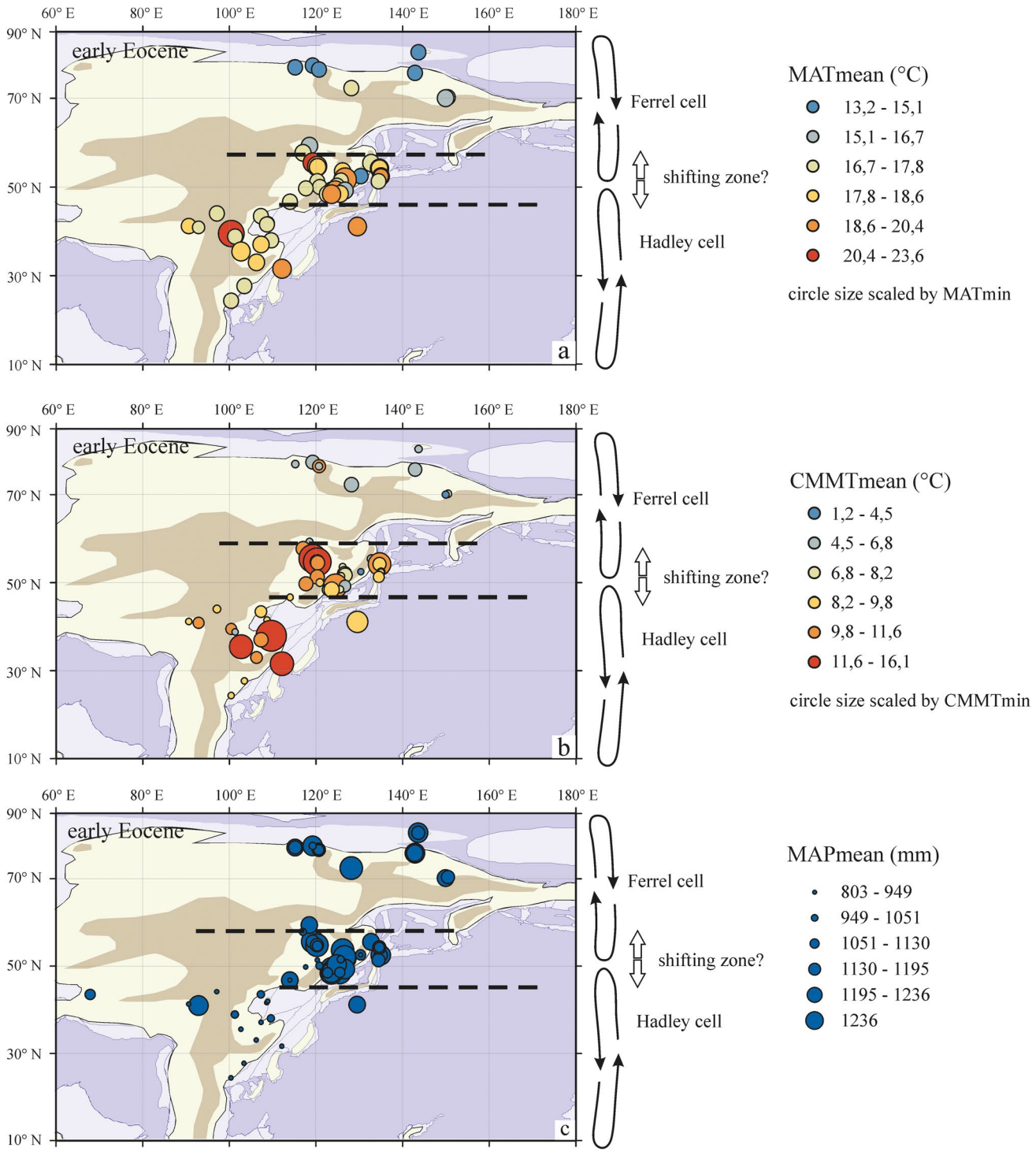

Fig. 7. Comparison of spatial distributions of MAT, CMMT and MAP along the Pacific side of Eurasia during the early Paleogene next to global atmospheric circulation

the 3WET/3DRY ratio, which for all assemblages return ratios near 4:1 for the early Late Cretaceous Arctic. For Amur Region Bondarenko et al. (2020b) indicate a MARP 148–238 mm in the early Palaeocene and 142–235 mm in the late Palaeocene. In the early Eocene of northern Yakutia (Eastern Siberia) the MARP varied from 107 to 247 mm in Lena River Delta (Bondarenko et al. 2022), and from 109 to 205 mm at Tastakh Lake (Bondarenko and Utescher 2023). According to Bondarenko et al. (2020a), the pronounced seasonality of precipitation of the Paleogene climate of

Primorye gradually increased from ca. 130 mm in the early Palaeocene to ca. 170 mm in the late Oligocene. According to Quan et al. (2012b), seasonal variability in precipitation in the early Paleogene of northeastern China appears to occur in most sites: summers were wet, with warm mean precipitation > 110 mm, whereas the winters were fairly dry with quite low precipitation (low mean precipitation < 35mm).

According to Spicer et al. (2019), the marked difference (near 4:1) in the 3WET/3DRY ratio obtained for all studied early Late Cretaceous assemblages of the Arctic suggests even more extreme rainfall seasonality than our early Paleogene values and that the Arctic may have experienced a "monsoonal" climate in the early Late Cretaceous. An essentially "summer wet" (wet/dry ratio 3:1) climate has been proposed for the Arctic in the Eocene, based on isotopic analysis of fossil wood interpreted to have been evergreen (Schubert et al. 2012), but an "ever wet" precipitation regime for this epoch is indicated by leaf form (West et al. 2015) based on predominantly deciduous angiosperm taxa.

The early Paleogene MARP was significantly higher than present. However, the much higher past MPwet coupled with distinctly higher MPdry indicate that during the early Paleogene the climate of Eastern Eurasia was significantly more humid. However, contrary to the distribution of MAP, MPdry and MPwet, where two zones are clearly distinguished – a wetter one to the north and a drier one to the south, with a transitional zone in between, the spatial pattern of MARP apparently was quite uniform (Fig. 5a-c).

Was there a monsoon in the early Paleogene after all?

The ratios of MPwet and MPdry to MAP are commonly used as indices of monsoon intensity in reconstructions based on of the palaeobotanical record (Jacques et al. 2014; Shukla et al. 2014; Spicer et al. 2014; West et al. 2015). According to Jacques et al. (2011a), the ratios of MPdry and MPwet to MAP are a good indication of past monsoon intensity (winter and summer, respectively). The monsoon is a complex climatic phenomenon, nevertheless, in general a decrease in RMPdry, i.e. a lower proportion of precipitation in the dry season, suggests the intensification of a winter monsoon, while an increase in RMPwet, i.e. higher proportion of precipitation in the wet season, may indicate the intensification of a summer monsoon.

For the early Paleogene of Eastern Eurasia, at high latitudes (north of 50° N palaeolatitude) the calculated proportions of MPdry (Fig. 6a-c) to yearly precipitation is half that of today, within ca. 40–50° N palaeolatitude the MPdry is similar to present-day, while to the south of 40° N palaeolatitude the proportion is 2–3 times higher than the modern one. For the calculated proportions of MPwet (Fig. 6d-f) to MAP, at high latitudes and up to ca. 40° N palaeolatitude the proportion is similar or a little higher compared to present-day, while to the south of 40° N palaeolatitude the proportion is half that of the modern one. The above described distribution of proportions in the early Paleogene along the Pacific coast of Eurasia suggests a more pronounced seasonality of precipitation at high latitudes and a less pronounced seasonality of precipitation in the mid-latitudes compared to present-day.

RMPwet is commonly considered a good proxy for EAM intensity (Jacques et al. 2011a). However, at high latitudes, precipitation seasonality cannot necessarily be explained by monsoon signals. Eldrett et al. (2014) associated seasonally wetter summers, existing shortly prior to and during the PETM interval in the North Sea, with enhanced hydrological cycling, a mechanism also operational in the Arctic during the late Cretaceous (Spicer and Herman 2010). RMPwet values calculated from our record could be interpreted in terms of a monsoonal type of climate. However, recent studies of modern monsoonal sites have shown that leaf physiognomy can be used in the identification of summer-precipitation-dominated monsoonal climates (Jacques et al. 2011b, 2014). This same signal may also be present in ecosystems that become dormant during the long dark winters of high latitude regions (Royer et al. 2003; Jahren and Sternberg 2008). Leaf area (LA) analysis estimates of MAP may be biased towards precipitation during the Arctic summer, as a result of the winter dormancy. The Arctic summer would have spanned 6–8 months in duration (West et al. 2015). Regions that exhibit monsoons, or "monsoon-type" summer-wet precipitation (RMPwet >55%; Zhang and Wang 2008) are not seasonally equable. Various types of monsoonal precipitation regimes have been proposed using both proxies and modelling data to characterise Eocene hyperthermal conditions in several regions of the Earth, including the Arctic and Antarctic (Huber and Goldner 2012; Schubert et al. 2012; Jacques et al. 2014). However, summer-wet precipitation regimes proposed for Polar Regions are in conflict with evidence from other proxies (Greenwood 1996; Eberle and Greenwood 2012). Estimates of seasonal precipitation from early Eocene megafloras of Ellesmere Island (Arctic Canada) by West et al. (2015) also contradict the monsoonal model, and rather are consistent with the modelling studies by Huber and Goldner (2012) that show Ellesmere Island and the surrounding region of the Arctic as "ever-wet". Schubert et al. (2012) applied isotopic analysis to fossilised wood from the High Arctic, using $\delta^{13}C$ to produce models that showed a high degree of seasonal precipitation: approximately 75% of the MAP falling during the summer polar light season. The dark polar winter as a result would have been comparatively dry. This high degree of seasonality, where the ratio of summer precipitation to MAP is greater than 55% (Zhang and Wang 2008), would imply a summer monsoonal precipitation regime for the early Eocene Arctic. However, LA analysis of the Arctic megafloras has produced MAP estimates that far

exceed the growing season precipitation estimates produced by the CLAMP analysis (West et al. 2015) while, for reasons cited above, LA analyses might not provide reliable results for High Arctic flora (see Herman 1994). Thus, at such high latitude, the revealed precipitation seasonality is not necessarily indicative of a monsoonal climate but could be explained by an enhanced hydrological cycle during the Arctic summers. Also, Eldrett et al. (2014) provide evidence for seasonally wetter summers shortly prior to and during the PETM interval in the North Sea and associate these shifts with enhanced hydrological cycling, a mechanism also operational in the Arctic during the Late Cretaceous that is supposed to cause high precipitation and humidity, under the presence of a permanent polar cloud cap (Spicer and Herman 2010).

The Paleogene pattern of the southern part of the Eurasian Pacific Coast (low and mid- latitudes) was possibly related to an early established monsoon-type circulation over East Asia (Quan et al. 2011, 2012a) and enhanced flow of humid air masses from the Pacific to inland areas of northeast Asia. Li et al. (2022) indicate that evolution and distribution of vegetation in East Asia during the Eocene, along with the global cooling, were triggered by monsoonal intensity, rain-shadow effects of the central and southwestern China highlands and basin extensions in the Pacific coastal realm to the east. According to Spicer et al. (2017), monsoonal climates at low latitudes (<32° N) in the early Eocene strongly depended on seasonal latitudinal migrations of the Intertropical Convergence Zone (ITCZ), continental configuration, orography and the strength of Hadley circulation.

Based on our reconstructions, and due to the fact that the highest values of RMPwet in the early Eocene do not exceed 25% even at mid-latitudes and, at the same time, vary within a narrow range and are evenly distributed over the study area – from 75 to 19° N (i.e. they do not show any latitudinal gradient), it can be assumed that our record cannot be interpreted in terms of a monsoonal type of climate. A main feature of the EAM is a dry cold season. The winter monsoon penetrates deeply into eastern Asia supported by a strong Siberian High (Molnar et al. 2010; Spicer et al. 2016). Today the Siberian High is a massive amount of cold dry air accumulating in the northeast of Eurasia from September until April. Its greatest size and strength is reached in the winter, with the air temperature lower than −40 °C in the centre of the high-pressure area (Dando 2005). According to Bondarenko and Utescher (2022), even the lowest values of the lower limits of the CIs for CMMTs in the early Eocene over Eastern Eurasia were not lower than −3.0 °C. Moreover, the early Paleogene palaeogeographic configuration of Asia fundamentally differed from modern (cf. Scotese 2013). The Tarim area and Siberian Platform were covered by a shallow epicontinental sea (Volkova and Kuz'mina 2005; Z. Zhang et al. 2007, 2012; Bosboom et al. 2014, 2015) that reduced the width in latitude of the continental area by about one quarter compared to present. During the early Paleogene, the maximum extent of marine transgression occurred in the mid-latitudes of Central Eurasia, with over 60% of the West Siberian Plate covered by water (Volkova and Kuz'mina 2005; Akhmetiev et al. 2012). Thus, it is most likely that the Siberian High, as one of the main drivers of the EAM monsoon system, did not yet exist in the early Eocene, at least not as a permanent feature.

When relying on monsoon indices based on climate variables derived from fossil floras it has to be considered that there are various other factors that strongly influence precipitation patterns, especially at low latitudes. Among these factors, Spicer et al. (2019) cite changes in the seasonal latitudinal migration of the ITCZ due to changes in the latitudinal temperature gradient. Therefore, monsoon indices should be used with caution. Another factor that may make it difficult to use rainfall patterns as an indicator of past monsoon intensity is the fact that most palaeobotanical records are preserved in basins where precipitation is commonly not the only source for humidity. This may introduce a bias towards humid conditions in palaeoclimate reconstructions (Spicer et al., 2019).

As regards the timing of the initiation of monsoon systems in east and southeast Asia, various authors suggest that the SAM existed as early as the Eocene (Licht et al. 2014; Shukla et al. 2014; Spicer et al. 2016; Bhatia et al. 2021a). More recent studies indicate that the palaeomonsoon in East Asia may have been initiated at lower latitudes, also in the course of the Eocene as is evident from coal and oil shale deposits along the southern margins of the subtropical arid zone (cf. Spicer et al. (2016, 2021) for a summary). Also, Li et al. (2022) relate changes in the spatial distribution of Eocene vegetation in East Asia to the influence of a monsoonal climate. As causes for the EAM initiation during the Eocene, enlargement of the continental area as a result of the Indo-Eurasia collision and uplifting of blocks in the realm of the present-day Tibetan Plateau can be cited (cf. An et al. 2015). Also, increased continentality of the climate related to the step-wise retreat of the Paratethys from the Tarim Basin since the middle Eocene (Bosboom et al. 2011) may have contributed to the initiation of the East Asian summer monsoon (EASM). Summarising these facts and according to the present results obtained we assume that the EAM system did not yet exist or was very weak in the earlier part of the Palaeogene and probably started to evolve at lower latitudes as summer monsoon (EASM) during the middle to late Eocene.

Distribution of dry and swamp elements

Fossil evidence for some genera may provide valuable clues about the regional early Paleogene climate and topography in the study area. Regarding rainfall, two contrasting groups of plants can be distinguished, such as dry (drought-resistant) and swamp taxa. In the early Paleogene floras of East Asia, *Ephedra* Mill. can be attributed to more-or-less widespread

dry taxa, while *Glyptostrobus pensilis* (Staunton ex D. Don) K. Koch and/or *Taxodium* Richard can be attributed to swamp elements. At present, *Ephedra* grows in arid regions throughout much of the Northern Hemisphere, including southern Europe, northern Africa, southwestern and central Asia, southwestern North America, and in the Southern Hemisphere, including South America south to Patagonia (Kharkevich 1989; FNA Editorial Committee 1993; Wu and Raven 1999). *Glyptostrobus* grows China, extinct in the wild in north Vietnam in river deltas, on flooded or waterlogged soil in full sun; near sea level (Wu and Raven 1999). *Taxodium* grows in North America, Mexico, Guatemala, in brownwater rivers, lake margins, and swamps, occasionally in slightly brackish water; 0–160 m (to 500 m) (Flora FNA Editorial Committee 1993). In China today *Taxodium* is used for afforestation on marshy soils (Wu and Raven 1999). As for the early Paleogene, distribution of modern constantly dry (Fig. 8a-c) and swamp elements (Fig. 8d-f), follows a precipitation gradient mirrored by MAP (Fig. 3a-c), MPdry (Fig. 4a-c) and MPwet (Fig. 4d-f).

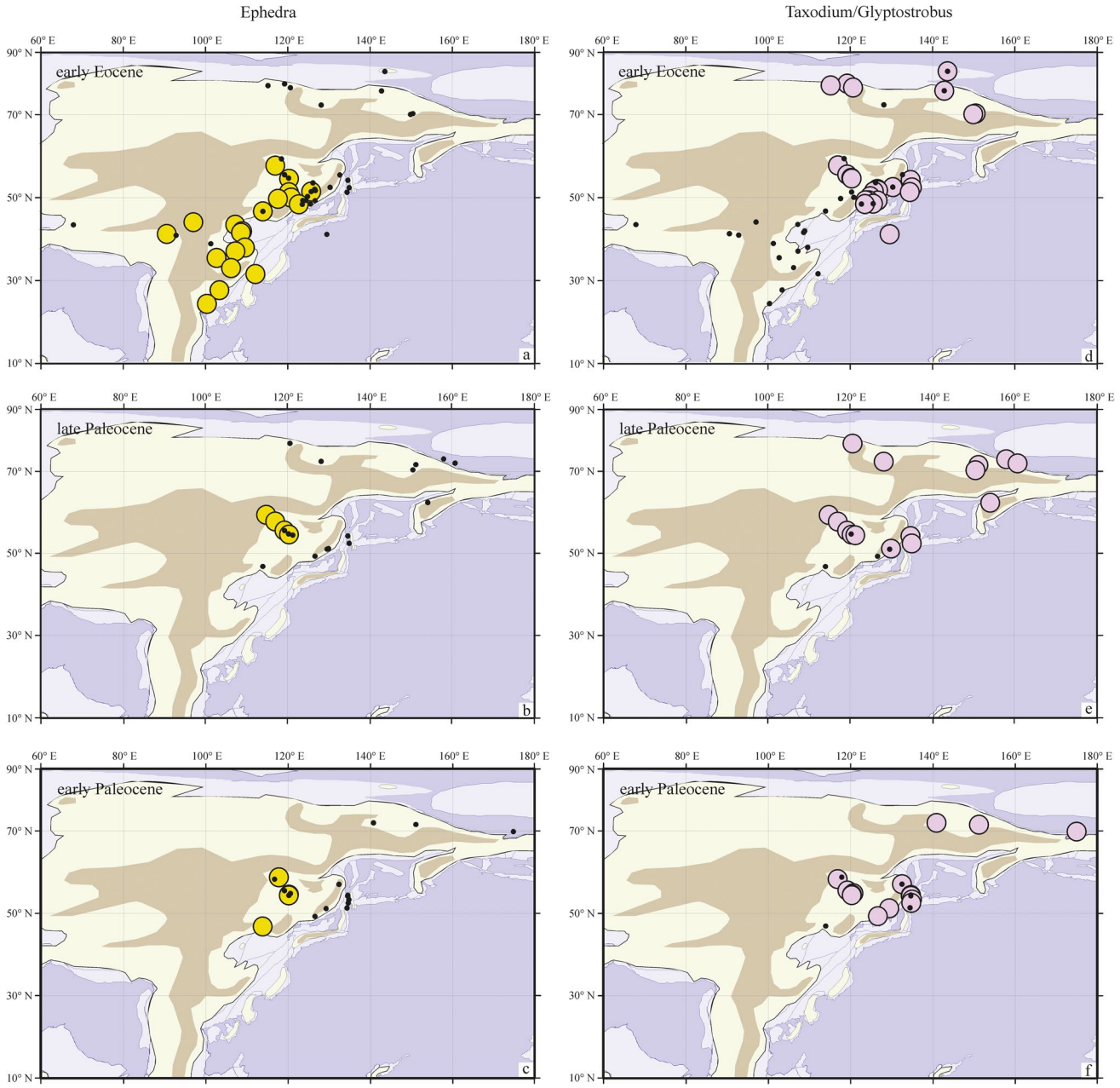

Fig. 8. Distribution of dry (*Ephedra*) and swamp (*Glyptostrobus*/*Taxodium*) elements along the Pacific side of Eurasia during the early Paleogene

In various earlier publications, East Asian Paleogene climates were subdivided into three latitudinal zones controlled by the planetary wind system (e.g. Liu 1997; Wang et al. 1999; Akhmetiev 2004; Guo et al. 2008; Z. Zhang et al. 2012). These zones are, at least partly, defined by hydrological constraints. Latitudinally, two humid zones located separately in the south and north are characterised by the occurrence of coals and/or oil shales, while the third broad arid zone resided in the middle and flanked by the two humid zones is largely reconstructed by the widespread red beds and/or evaporites along ca. 30° N palaeolatitude (ranging between ~25° N and ~35° N), allegedly driven by the then subtropical highs (Liu 1997; Wang et al. 1999; Guo et al. 2008; Z. Zhang et al. 2012). The northern humid zone, characterised by coals and/or oil shales, is well correlated with our wetter zone located to north of 50° N palaeolatitude. The broad "arid" zone in the mid-latitudes and is largely recognised by the widespread red beds and/or evaporates, corresponds to our drier zone located to south of 50° N palaeolatitude.

Based on Plant Functional Type (PFT) vegetation reconstruction of east Asian palaeofloras, Li et al. (2022) suggest the expansion of humid broadleaved forest from the southeast, as well as the retreat of dry shrub and open woodland from the northwest during the early to late Eocene. These reconstructed vegetation patterns have been related to the continental distribution of rainfall and are supported by mammal distribution, lithological indicators, and geochemical proxies. Moreover, the resulting vegetation pattern shows largely east-west differentiation and absence of tropical vegetation from southern China during the Eocene (Li et al. 2022). The reconstructed early Eocene vegetation pattern coincides with our results showing a declining MAP gradient from the eastern coastal areas to the western continental inland region.

Conclusions

For the first time, a comprehensive quantitative palaeoprecipitation data set has been compiled for the Pacific side of Eurasia for the early Paleogene. The results obtained fill a regional gap in currently available datasets for Eurasia, with a focus on Russian Far East and Eastern Siberia, where data paucity seriously hinders their understanding in a global context. Based on the consistent analysis of 110 floras, for the first time detailed spatial gradients and temporal trends in precipitation changes along the Pacific coast of Eurasia in the early Paleogene are quantified.

The early and late Palaeocene precipitation gradients were very weak. Based on means of MAP data, a minor gradient is observed between the southern and northern sectors at 50° N. In the early Eocene, the MAP gradient became more clearly pronounced, and a larger "arid" zone can be distinguished in the mid-latitudes. The early Eocene MAP gradients are basically NW-SE oriented. Generally, our data show a higher level of MAP, MPdry and MPwet for the high and higher mid-latitudes of the Pacific areas of Eurasia in the early Paleogene compared to the present-day. This correlates well with higher MAT, CMMT, and WMMT values, as well as with latitudinal temperature gradients of the Pacific side of Eurasia in the early Eocene.

Our reconstruction demonstrates a clear regional subdivision (especially pronounced in the early Eocene) into two zones located to the north and south of ca. 50° N palaeolatitude, as expressed by MAP, MPdry and MPwet data. Between both zones, within the range of ca. 5° to south and north from 50° N palaeolatitude, a transition zone can be distinguished where the presence of floras existing under higher and lower values of all precipitation parameters is observed.

Our data suggest that in the early Paleogene, the global atmospheric circulation consisted of two well-defined cells, Hadley and Ferrell, while the polar cell was either absent or located over the Arctic Ocean and was very weak. This explains the presence of a drier zone to the south and a wetter zone to the north. It seems that the boundary between the Hadley and Farrell cells ran at about 50° N palaeolatitude, while the transition zone could reflect the possible shorter-term migration/shifting area of these cells. The asymmetric (NW-SE) orientation of these two zones is mirrored the northward energy transport by ocean and atmosphere.

Due to the fact that the highest RMPwet values in our early Eocene reconstruction did not exceed 25%, even at mid-latitudes and, at the same time, vary within a narrow range and are evenly distributed over the territory studied (i.e. they do not show any latitudinal gradient), it can be assumed that our record cannot be interpreted in terms of a monsoonal type of climate.

The distribution of swamp taxa (*Glyptostrobus* and *Taxodium*) is well correlated with our wetter zone located to the north of 50° N palaeolatitude and distribution of coals and/or oil shales. The distribution of the dry taxon (*Ephedra*) corresponds to our drier zone located to south of 50° N palaeolatitude and coincides with the regional distribution of red bed sediments and/or evaporites.

Supplementary Information The online version contains supplementary material available at https://doi.org/10.1007/s12549-023-00586-y.

Acknowledgements This work was supported by the Russian Science Foundation No. 22-27-00098, https://rscf.ru/project/22-27-00098/. Partly, as a study of the climate of some single Palaeocene and early Eocene locations of Yakutia, Amur River Region and Primorye, the research was carried out within the state assignment of Ministry of Science and Higher Education of the Russian Federation (theme No. 121031500274-4). The authors are grateful to Prof. Dr. Gaurav Srivastava and an anonymous reviewer for carefully revising the manuscript and for their valuable suggestions. The authors are grateful to Alan Lord for language checking, and Editor-in-Chief Dieter Uhl and Managing

Editor Sinje Weber for constructive comments and help. The authors thank T.A. Evstigneeva, A.A. Zhmerenetsky and R.Z. Allaguvatova (Federal Scientific Center for Biodiversity, FEB RAS) for help with the collection and verification of the published original paleobotanical material for the Pacific coast of Eurasia in the early Paleogene, as well as the clarification of the nearest living relatieves for fossil taxa and their reliability within the framework of the Russian Science Foundation project No. 22-27-00098. This work contributes to NECLIME (Neogene Climate Evolution in Eurasia).

Funding Open Access funding enabled and organized by Projekt DEAL.

Data availability All data generated or analysed during this study are included in this published article and its supplementary information files.

Compliance with ethical standards

Conflict of interest The authors declare that they have no conflict of interest.

References

Abels, H.A., Dupont-Nivet, G., Xiao, G., Bosboom, R., & Krijgsman, W. (2011). Step-wise change of Asian interior climate preceding the Eocene – Oligocene Transition (EOT). *Paleogeography, Paleoclimatology, Paleoecology 299*, 399–412.

Ablaev, A.G. (1976). An excursion into the early Cenozoic history of the geological development of the West Sakhalin sedimentary basin, In A. G. Ablaev (Ed.), *Essays on the geology and paleontology of the Far East* (pp. 15–19). Vladivostok: Far Eastern Scientific Center of the Academy of Sciences of the USSR. [in Russian]

Ablaev, A.G., Li, C.S., Vasiliev, I.V., & Wang, Y.F. (2005). *Paleogene of the eastern Sikhote-Alin* (pp.1- 95). Vladivostok: Dal'nauka,. [in Russian]

Akhmetiev, M.A. (1973). Paleocene and Eocene flora of the southern Far East of the USSR and adjacent countries and their stratigraphic position. *Sovetskaya geologiya 7*, 14–29. [in Russian]

Akhmetiev, M.A. (1988). *Cenozoic flora of eastern Sikhote-Alin* (pp. 48). Moscow: Geologicheskii institut Akademii nauk SSSR. [in Russian]

Akhmetiev, M.A. (1993). *Phytostratigraphy of Paleogene and Miocene continental deposits of Boreal Asia* (Transactions of the Geological Institute of the Russian Academy of Sciences 475). Moscow: Nauka. [in Russian]

Akhmetiev, M.A. (2004). The Paleocene and Eocene Global Climate. Paleobotanical evidences, In M.A. Semikhatov, N.M. Chumakov (Eds.), *Climate in the Epoches of Major Biospheric Transformations* (pp. 10–43). (Trudy Geologicheskogo Instituta RAN, Vol. 550). Moscow: Geologicheskii institute Rossiiskoi akademii nauk. [in Russian]

Akhmetiev, M.A. (2015). High-latitude regions of Siberia and northeast Russia in the Paleogene: stratigraphy, flora, climate, coal accumulation. *Stratigraphy and Geological Correlation 23(4)*, 421–435.

Akhmetiev, M.A., & Golovneva, L.B. (1998). New data on the composition and age of the Malomikhailovskaya flora (Upper Cretaceous, Lower Amur Region). *Stratigraphy and Geological Correlation 6(3)*, 43–55. [in Russian]

Akhmetiev, M., Walther, H., & Kvaček, Z. (2009). Mid-latitude Palaeogene floras of Eurasia bound to volcanic settings and palaeoclimatic events – experience obtained from the Far East of Russia (Sikhote-Alin) and Central Europe (Bohemian Massif). *Acta Musei Naturalis Pragae, Series B, Historia Naturalis 65*, 61–129.

Akhmetiev, M.A., & Zaporozhets, N.I. (2017). The climate-forming role of early Paleogene marine currents in high latitudes of Eurasia. *Stratigraphy and Geological Correlation 25*, 229–239.

Akhmetiev, M.A., Zaklinskaya, E.D., & Medyulyanov, V.I. (1978). Paleobotanical characteristics of the Danian, Paleocene and Lower Eocene deposits of Western Sakhalin. *Sovetskaya Geologiya 5*, 77–89. [in Russian]

Akhmetiev, M.A., Zaporozhets, N.I., Benyamovskiy, V.N., Aleksandrova, G.A., Iakonleva, A.I., & Oreshkina, T.V. (2012). The Paleogene history of the Western Siberian seaway – a connection of the Peri-Tethys to the Arctic Ocean. *Austrian Journal of Earth Sciences 105(1)*, 50–67.

Amiot, R., Lecuyer, C., Beuffetaut, E., Frederic, F., Legendre, S., & Meartineau, F. (2004). Latitudinal temperature gradient during the Cretaceous Upper-Campanian – Middle Maastrichtian: $\delta^{18}O$ record of continental vertebrates. *Earth and Planetary Science Letters 226(1-2)*, 255–272.

An, W., Hu, X., Garzanti, E., Wang, J.G., & Liu, Q. (2021). New precise dating of the India-Asia collision in the Tibetan Himalaya at 61 Ma. *Geophysical Research Letters 48*, e2020GL090641.

An, Z.S. (2000). The history and variability of the East Asian paleomonsoon climate. *Quaternary Science Reviews 19*, 171–87.

An, Z.S., Kutzbach, J.E., Prell, W.L., & Porter, S.C. (2001). Evolution of asian monsoons and phased uplift of the himalayan – Tibetan plateau since late Miocene times. *Nature 411*, 62–66.

An, Z.S., Sun, Y.B., Chang, H., Zhang, P.Z., Liu, X.D., & et al. (2014). Late Cenozoic climate in monsoon-arid Asia and global changes. In Z. S. An (Ed.), *Late Cenozoic Climate Change in Asia: Loess, Monsoon and Monsoon-Arid Environment Evolution* (pp. 491–582). Springer.

An, Z.S., Wu, G.X., Li, J.P., Sun, Y.B., Liu, Y., Zhou, W.J., Cai, Y.J., Duan, A.M., Li, L., Mao, J.G., Cheng, H., Shi, Z.G., Tan, L.C., Yan, H., Ao, H., Chang, H., & Feng, J. (2015). Global monsoon dynamics and climate change. *Annual Review of Earth and Planetary Sciences 43*, 29–77.

Baikovskaya, T.N. (1950). Paleocene flora of the Zee-Bureya Plain. *Voprosy paleontologii 1*, 348–381. [in Russian]

Baskakova, L.A., & Gromova, N.S. (1979). Biostratigraphic dismemberment of the Uglovskii horizon according to palynological data, In B. V. Poyarkov (Ed.), *Paleontology and stratigraphy of the Far East* (pp. 109–114). Vladivostok: Dal'nevostochnyi nauchnyi tsentr Akademii nauk SSSR. [in Russian]

Baskakova, L.A., & Gromova, N.S. (1984). Stratigraphy of Smolyaninovskii coal mine in the Southern Primorye, In A. G. Ablaev (Ed.), *Materials on stratigraphy and paleogeography of East Asia* (pp. 59–69). Vladivostok: Dal'nevostochnyi nauchnyi tsentr Akademii nauk SSSR. [in Russian]

Baskakova, L.A., & Lepekhina, V.G. (1990). New data on the phytostratigraphy of the Paleogene of the Zerkal'nenskii Basin, In A. G. Ablaev (Ed.), *New data on stratigraphy of the Far East and the Pacific Ocean* (pp. 52–60). Vladivostok: Dal'nevostochnoe otdelenei Rossiiskoi akademii nauk. [in Russian]

Belaya, B.V., & Litvinenko, I.S. (1988). Structure and age of Cenozoic sediments in the Khatakhan - Yarovaya interfluve (Anui

depression). In V. I. Volobueva, (Ed.), *Continental Paleogene and Neogene of the Northeast of the USSR* (pp. 18–32). Issue 3. Chukotka. Magadan: Izdatel'stvo SVKNII DVO AN SSSR. [in Russian]

Bhatia, H., Khan, M.A., Srivastava, G., Hazra, T., Spicer, R.A., Hazra, M., Mehrotra, R.C., Spicer, T.E.V., Bera, S., & Roy, K. (2021a). Late Cretaceous – Paleogene monsoon climate via-à-vis movement of the Indian plate, and the birth of the south Asia monsoon. *Gondwana Research 93*, 89–100.

Bhatia, H., Srivastava, G., Spicer, R.A., Farnsworth, A., Spicer, T.E.V., Mehrotra, R.C., Paudayal, K.N., & Valdes, P. (2021b). Leaf physiognomy records the Miocene intensification of the south Asia monsoon. *Global and Planetary Change 196*, 103365.

Bhatia, H., Srivastava, G., Adhikan, P., Su, T., Utescher, T., Paudayal, K.N., & Mehrotra, R.C., (2022). Asian monsoon and vegetation shift: evidence from the Siwalik succession of India. *Geological Magazine 159*, 1397-–1414.

Bijl, P.K., Schouten, S., Sluijs, A., Reichart, G.-J., Zachos, J.C., & Brinkhuis, H. (2009). Early Palaeogene temperature evolution of the southwest Pacific Ocean. *Nature 461*, 776–779.

Bolotnikova, M.D. (1977). Palynocomplex of the Khulgunskaya Formation of the Tigilsky Reference Section (Western Kamchatka), In V. A. Krassilov (Ed.), *Paleobotany in the Far East* (pp. 38–44) Vladivostok: Far Eastern Scientific Center of the AN USSR. [in Russian]

Bolotnikova, T.N. (1988). Palynological characteristics and age of coal-bearing deposits of the Chernyshevskii Brown Coal Field (Southern Primorye). *Tikhookeanskaya geologia 4*, 101–105. [in Russian]

Bondarenko, O.V., & Utescher, T. (2022). Early Paleogene continental temperature patterns and gradients over eastern Eurasia. *Journal of Asian Earth Sciences 239*, 105401.

Bondarenko, O.V., & Utescher, T. (2023). Late early to early middle Eocene climate and vegetation change at Tastakh Lake (northern Yakutia, Eastern Siberia). *Palaeobiodiversity and Palaeoenvironments 103*(2), 277–301.

Bondarenko, O.V., Blokhina, N.I., Mosbrugger, V., & Utescher, T. (2020a). Paleogene climate dynamics in the Primorye Region, Far East of Russia, based on a Coexistence Approach analysis of palaeobotanical data. *Palaeobiodiversity and Palaeoenvironments 100*(1), 5–31.

Bondarenko, O.V., Utescher, T., Blokhina, N.I., Evstigneeva, T.A., & Kezina, T.V. (2020b). Temporal climate and vegetation gradient of the Paleocene in the Amur Region (Far East of Russia). *Botanica Pacifica 9(2)*, 13–35.

Bondarenko, O.V., Blokhina, N.I., Evstigneeva, T.A., & Utescher, T. (2022). Short-term climate and vegetation dynamics in Delta Lena River (northern Yakutia, Eastern Siberia) during the early Eocene. *Palaeoworld 31*(3), 521–541.

Borsuk, M.O. (1952). *Fossil flora of the Upper Cretaceous sediments of Primorye* (pp. 1-52). Vladivostok: Gosgeoltekhizdat. [in Russian]

Bosboom, R.E., Dupont-Nivet, G., Houben, A.J.P., Brinkhuis, H., Villa, G., Mandic, O., Stoica, M., Zachariasse, W.-J., Guo, Z., & Li, C. (2011). Late Eocene sea retreat from the Tarim Basin (west China) and concomitant Asian paleoenvironmental change. *Palaeogeography, Palaeoclimatology, Palaeoecology 299*, 385–398.

Bosboom, R.E., Abels, H.A., Hoorn, C., van den Berg, B.C.J., Guo, Z., & Dupont-Nivet, G. (2014). Aridification in continental Asia after the Middle Eocene Climatic Optimum (MECO). *Earth and Planetary Science Letters 389*, 34–42.

Bosboom, R., Mandic, O., Dupont-Nivet, G., Proust, J.N., Ormukov, C., & Aminov, J. (2015). Late Eocene palaeogeography of the proto-Paratethys Sea in Central Asia (NW China, southern Kyrgyzstan and SW Tajikistan), In M. F. Brunet, T. McCann, E. R. Sobel (Eds.), *Geological Evolution of Central Asian Basins and the Western Tien Shan Range* (Special Publications) (pp. 427). London: Geological Society.

Brattseva, G.M. (1969). *Palynological studies of upper Cretaceous and Paleogene of the Far East*. Geological Institute Transactions. Academy of Sciences USSR 207, 1–57. [in Russian]

Breedlovestrout, R.L., Evraets, B.J., & Parrish, J.T. (2013). New Paleogene palaeoclimate analysis of western Washington using physiognomic characteristics from fossil leaves. *Palaeogeography, Palaeoclimatology, Palaeoecology 392*, 22–40.

Bruch, A.A., Utescher, T., Mosbrugger, V., & NECLIME members. (2011). Precipitation patterns in the Miocene of Central Europe and the development of continentality. *Palaeogeography, Palaeoclimatology, Palaeoecology 304*, 202–211.

Budantsev, L.Yu. (1983). *History of the Arctic flora of the early Kainophytic era* (pp.*1*-156). Saint Petersburg: Nauka. [in Russian]

Budantsev, L.Yu. (1999). The reconstruction of the Cenozoic climates in eastern-north Asia based on palaeobotanical data. *Botanicheskii Zhurnal 84*(10), 36–45. [in Russian]

Caley, T., Malaiz´e, B., Revel, M., Ducassou, E., Wainer, K., Ibrahim, M., Shoeaib, D., Migeon, M., & Marieu, V. (2011). Orbital timing of the Indian, East Asian and African boreal monsoons and the concept of a "global monsoon." *Quaternary Science Reviews 30*, 3705–3715.

Chekryzhov, I.Yu., Popov, V.K., Panichev, A.M., Seredin, V.V., & Smirnova, E.V. (2010). New data on stratigraphy, volcanism, and zeolite mineralization of the Cenozoic Vanchinskii Basin, Primorsky Krai. *Tikhookeanskaya geologia 29*(4), 45–63. [in Russian]

Chen, J., Gao, Y., Ibarra, D.E., Qin, J.M., & Wang, C.S. (2022). Mid-latitude precipitation in East Asia influenced by a fluctuating greenhouse climate during the latest Cretaceous through the earliest Paleogene. *Global and Planetary Change 216*, 103900.

Chen, P.J., Wan, X.Q., Jiang, J.H., Li, X.H., Cao, L., Li, G., Liu, J.C., Yin, D.S., Yan, W., & Li, W.X. (2004). Searching for the stratotype of the Furao stage in Heilongjiang Province, Northeast China. *Journal of Stratigraphy 28*(2), 97–104.

Cheng, H., Sinha, A., Wang, X.F., Cruz, F.W., & Edwards, R.L. (2012). The global paleomonsoon as seen through speleothem records from Asia and the Americas. *Climate Dynamics 39*, 1045–1062.

Clemens, S.C., Prell, W.L., & Sun, Y. (2010). Orbital-scale timing and mechanisms driving Late Pleistocene Indo-Asian summer monsoons: reinterpreting cave speleothem $\delta^{18}O$. *Paleoceanography 25*, PA4207.

Cohen, K.M., Finney, S.M., Gibbard, P.L., & Fan, J.X. (2013). The ICS International Chronostratigraphic Chart. *Episodes 36*, 199–204.

Dando, W.A. (2005). Asia. Climates of Siberia, Central and East Asia, In J.E. Oliver (Ed.), *Encyclopedia of World Climatology* (pp. 102–114). Dordrecht: Springer.

Dupont-Nivet, G., Krijgsman, W., Langereis, C., Abels, H.A., Dai, S., & Fang, X. (2007). Tibetan plateau aridification linked to global cooling at the Eocene–Oligocene transition. *Nature 445*, 635–638.

Eberle, J.J., & Greenwood, D.R. (2012). Life at the top of the greenhouse Eocene world – a review of the Eocene flora and vertebrate fauna from Canada's High Arctic. *Geological Society of America Bulletin 124*, 3–23.

Eldrett, J.S., Greenwood, D.R., Harding, I.C., & Huber, M. (2009). Increased seasonality through the Eocene to Oligocene transition in northern high latitudes. *Nature 459*, 969–973.

Eldrett, J.S., Greenwood, D.R., Polling, M., Brinkhuis, H., & Sluijs, A. (2014). A seasonality trigger for carbon injection at the Paleocene–Eocene thermal maximum. *Climate of the Past 10*, 1–11.

Fan, M., (1985). Spore-pollen assemblages of Paleocene Xinancun formation in Shulan Coalfield. *Coal Technology of Northeast China 3*, 13–26. [in Chinese]

Fang, J., Wang, Z., & Tang, Z. (2009). *Atlas of Woody Plants in China*. Vol. 1 and Index. Beijing: Higher Education Press.

Fang, J., Wang, Z., & Tang, Z. (2011). *Atlas of Woody Plants in China*. Vol. 2 and Index. Beijing: Higher Education Press.

Farnsworth, A., Lunt, D.J., Robinson, S.A., Valdes, P.J., Roberts, W.H.G., Clift, P.D., Markwick, P., Su, T., Wrobel, N., Bragg, F., Kelland, S.-J., & Pancost, R.D. (2019). Past East Asia monsoon evolution controlled by paleogeography, not CO_2. *Science Advances 5*, eaas1697.

Fedotov, V.V. (1983). *Eocene flora of Raychikha of the Amur region* (pp.1-287). Vol. 1 and 2. (Dep. VINITI No. 2774-83). [in Russian]

FNA Editorial Committee (Eds.), (1993). *Flora of North America North of Mexico* (pp.*1*-496). vol. 2 (Pteridophytes and Gymnosperms). Oxford: Oxford University Press.

Fotjanova, L.I., Serova, M.Ya., Gal'versen, V.G., Zharov, A.E., Grokhotova, N.M., & Tuzov, V.P. (2001). The Paleogene Reference section of the Kril'on Peninsula (the Kitosiya River, Southern Sakhalin). *Stratigraphy and Geological Correlation 9(2)*, 58–76. [in Russian]

Fradkina, A.F. (1985). Paleogene and Neogene of the lower reaches of the Kolyma River according to palynological data, In V.S. Volkova, A.F. Fradkina (Eds.), *Palynostratigraphy of the Mesozoic and Cenozoic of Siberia* (pp. 52–65). (Transactions of Instituta geologii i geofiziki RAN, Vol. 620). Novosibirsk: Nauka. [in Russian]

Fradkina, A.F. (1995). *Palynostratigrapy of Paleogene and Neogene Sediments of North-Eastern Russia* (pp.1-82). (Transactions of the UIGGM SB RAS, Vol. 806). Novosibirsk: Nauchno-izdatel'skii tsentr OIGGiM SO RAN. [in Russian]

Fradkina, A.F., & Laukhin, S.A. (1984). A brief palynological characteristic of the Paleogene in the Lower Kolyma and the problem of the Eocene-Oligocene boundary in Northeast Asia, In S. B. Shatskii, V. S.Volkova, & I. A. Kulkova (Eds.), *Environment and life at the boundaries of the Cenozoic eras in Siberia and the Far East* (pp. 34–41). (Transactions of Instituta geologii i geofiziki, Vol. 593). Novosibirsk: Nauka. [in Russian]

Fradkina, A.F., Trufanov, G.V., & Vakulenko, A.S. (1979). Eocene Deposits of New Siberian islands, In N.A. Schilo, Yu.P. Baranova (Eds.), *Continental Tertiary deposits of North-East Asia* (*Stratigraphy, Correlation, Paleoclimates*) (pp. 22–30*)*. Novosibirsk: Nauka. [in Russian]

Gladenkov, Yu.B., Bazhenova, O.K., Grechin, V.I., Margulis, L.S., & Salnikov, B.A. (2002). *The Cenozoic Geology and the Oil and Gas Presence in Sakhalin* (pp.1–225). Moscow: GEOS. [in Russian]

Gladenkov, Yu.B., Sinel'nikova, V.N., Chelebaeva, A.I., & Shantser, A.E. (2005). *Biosphere – Ecosystem – Biota in the Earth Past. The North Pacific Cenozoic ecosystems: Eocene – Oligocene of West Kamchatka and adjacent regions* (pp. 1–480) (To the centenary of Academician V.V. Menner). Transactions of the Geological Institute, Vol. 540. Moscow: GEOS. [in Russian]

Goswami, B.N., Krishnamurthy, V., & Annamalai, H. (1999). A broad-scale circulation index for interannual variability of the Indian summer monsoon. *Quarterly Journal of the Royal Meteorological Society 125*, 611–633.

Greenwood, D.R. (1996). Eocene monsoon forests in central Australia? *Australian Systematic Botany 9*, 95–112.

Greenwood, D.R., & Wing, S.L. (1995). Eocene continental climates and latitudinal temperature gradients. *Geology 23*, 1044–1048.

Greenwood, D.R., Basinger, J.F., & Smith, R.Y. (2010). How wet was the Arctic Eocene rain forest? Estimates of precipitation from Paleogene Arctic macrofloras. *Geology 38*, 15–18.

Greenwood, D.R., Pigg, K.B., & DeVore, M.L. (2016). Eocene paleontology and geology of western North America. *Canadian Journal of Earth Sciences 53*, 543–547.

Grinenko, O.V., & Fradkina, A.F. (1988). Palynological characteristics of the Paleogene deposits of the Northern Kharaulakh, In V.S. Volkova, S.B. Shatskii, (Eds.), *Microphytofossils and stratigraphy of the Mesozoic and Cenozoic of Siberia* (pp. 136–142). Transactions of Institut Geologii i Geofiziki, Sibirskoe otdelenie, Akademiya. Nauk SSSR, Vol. 697. Novosibirsk: Nauka. [in Russian]

Grinenko, O.V., & Kiseleva, A.V. (1971). On the age of coal-bearing deposits of the Bykovskaya channel in the delta of the Lena River, In A.I. Tomskaya, & V.F. Vozin, (Eds.), *Palynological characteristics of Paleozoic, Mesozoic and Cenozoic deposits of Yakutia* (pp. 75–87). Yakutsk: Yakutskoe knizhnoe izdatel'stvo. [in Russian]

Grinenko, O.V., Zharikova, L.P., Fradkina, A.F., & et al. (1989). *The Paleogene and Neogene of the North-Eastern USSR* (pp. 1-184). Yakutsk: Yakut Scientific Center SB AS USSR. [in Russian]

Grinenko, O.V., Sergeenko, A.I., & Belolubskiy, I.N. (1997). Stratigraphy of the Paleogene and Neogene deposits of the North-East of Russia. *Otechestvennaya geologiya 8*, 14–20. [in Russian]

Gu, C., & Renaut, R.W. (1994). The effect of Tibetan uplift on the formation and preservation of Tertiary lacustrine source-rocks in eastern China. *Journal of Paleolimnology 11*, 31–40.

Guo, Z.-T., Sun, B., Zhang, Z.-S., Peng, S.-Z., Xiao, G.-Q., Ge, J.-Y., Hao, Q.-Z., Qiao, Y.-S., Liang, M.-Y., Liu, J.-F., Yin, Q.-Z., & Wei, J.-J. (2008). A major reorganization of Asian climate by the early Miocene. *Climate of the Past 4*, 153–174.

Hao, H., Ferguson, D.K., Feng, G.P., Ablaev, A., Wang, Y.F., & Li, C.S. (2010). Early Paleocene vegetation and climate in Jiayin, NE China. *Climate Change 99*, 547–566.

He, Y.M., & Sun, X.J. (1977). Palynological investigation of Palaeogene in the Qingjiang Basin in Kiangsi Province I. *Acta Botanica Sinica 19*, 72–82.

He, C.X., & Tao, J.R. (1997). A study on the Eocene flora in Yilan County, Heilongjiang. *Acta Phytotaxonomica Sinica 35*, 249–256.

Herman, A.B. (1994). Late Cretaceous Arctic platanoids and high latitude climate. In M.C. Boulter, & H.C. Fisher (Eds.), *Cenozoic Plants and Climates of the Arctic* (pp. 151–159). Berlin, Heidelberg: Springer.

Herman, A.B., & Spicer, R.A. (1996). Palaeobotanical evidence for a warm Cretaceous Arctic Ocean. *Nature 380*, 330–333.

Herman, A.B., & Spicer, R.A. (1997). New quantitative palaeoclimate data for the Late Cretaceous Arctic: evidence for a warm polar ocean. *Palaeogeography, Palaeoclimatology, Palaeoecology 128*, 227–251.

Herman, A.B., Golovneva, L.B., Shczepetov, S.V., & Grabovsky, A.A. (2016). The late Cretaceous Arman Flora of Magadan oblast, Northeastern Russia. *Stratigraphy and Geological Correlation 24*, 651–760.

Herold, N., Buzan, J., Seton, M., Goldner, A., Green, J.A.M., Müller, R.D., Markwick, P., & Huber, M. (2014). A suite of early Eocene (55 Ma) climate model boundary conditions. *Geoscientific Model Development 7*, 2077–2090.

Hong, Y.C., Yang, Z.Q., Wang, S.T., Sun, X.J., Du, N.Q., Sun, M.R., & Li, Y.G. (1980). *A Research on the Strata and Palaeontology of the Fushun Coal Field in Liaoning Province*. Beijing: Science Press.

Hoorn, C., Straathof, J., Abels, H.A., Hu, Y.D., Utescher, T., & Dupont-Nivet, G. (2012). A late Eocene palynological record of climate change and Tibetan Plateau uplift (Xining Basin, China). *Palaeogeography, Palaeoclimatology, Palaeoecology 344-345*, 16–38.

Huang, J.L., & McElroy, M.B. (2014). Contributions of the Hadley and Ferrel circulations to the energetic of the atmosphere over the past 32-years. *Journal of Climate 27*, 2656–2666.

Huber, B.T., & Goldner, A. (2012). Eocene monsoons. *Journal of Asian Earth Sciences 44*, 3–23.

Jacques, F.M.B., Guo, S.X., Su, T., Xing, Y.-W., Huang, Y.-J., Liu, Y.S. (Ch.), Ferguson, D.K., & Zhou, Z.-K. (2011a). Quantitative reconstruction of the late Miocene monsoon climates of southwest China: A case study of the Lincang flora from Yunnan Province. *Palaeogeography, Palaeoclimatology. Palaeoecology 304*, 318–327.

Jacques, F.M.B., Su, T., Spicer, R.A., Xing, Y., Huang, Y., Wang, W., & Zhou, Z. (2011b). Leaf physiognomy and climate: are monsoon systems different? *Global and Planetary Change 76*, 56–62.

Jacques, F.M.B., Su, T., Spicer, R.A., Xing, Y.-W., Huang, Y.-J., & Zhou, Z.-K. (2014). Late Miocene southwestern Chinese floristic diversity shaped by the southeastern uplift of the Tibetan Plateau. *Palaeogeography, Palaeoclimatology. Palaeoecology 411*, 208–215.

Jahren, A.H., & Sternberg, L.S. (2008). Annual patterns within tree rings of the Arctic middle Eocene (ca. 45 Ma): isotopic signatures of precipitation, relative humidity, and deciduousness. *Geology 36*, 99–102.

Jin, J.H., Herman, A.B., Spicer, R.A., & Kodrul, T.M. (2017). Palaeoclimate background of the diverse Eocene floras of South China. *Science Bulletin 62*, 1501–1503.

Johnson, K.R., & Ellis, B. (2002). A tropical rainforest in Colorado 1.4 million years after the Cretaceous – Tertiary boundary. *Science 296*, 2379–2383.

Jolley, D.W., & Widdowson, M. (2005). Did Paleogene North Atlantic rift-related eruptions drive early Eocene climate cooling? *Lithos 79*, 355–366.

Kalishevich, T.G., Zaklinskaya, E.D., & Serova, M.Ya. (1981). *Development of the organic world of the Pacific belt at the turn of the Mesozoic and Cenozoic* (pp. *1*-164). Moscow: Nauka. [in Russian]

Kalnay, E., Kanamitsu, M., Kistler, R., Collins, W., Deaven, D., Gandin, L., Iredell, M., Saha, S., White, G., Woollen, J., Zhu, Y., Leetmaa, A., Reynolds, B., Chelliah, M., Ebisuzaki, W., Higgins, W., Janowiak, J., Mo, K.C., Ropelewski, C., Wang, J., Jenne, R., & Joseph, D. (1996). The NCEP/NCAR 40-year reanalysis project. *Bulletin of the American Meteorological Society 77*, 437–471.

Kamaeva, A.M. (1990). *Stratigraphy and flora of the boundary deposits of Cretaceous and Paleogene of the Zeya-Bureya Depression* (pp. 1- 65). Khabarovsk: Amur Integrated Research Institute DVO AN SSSR. [in Russian]

Kezina, T.V. (1997). Palinostratigraphy of the Maastrichtian-Danian deposits of the Pikanskii Basin (Amur region). *Tikhookeanskaya geologia 16*, 140–142. [in Russian]

Kezina, T.V. (2005). *Palynostratigraphy of coal deposits of the Late Cretaceous and Cenozoic of the Upper Amur River Region* (pp. *1*-206). Vladivostok: Dal'nauka. [in Russian]

Kezina, T.V., & Litvinenko, N.D. (2007). Palynostratigraphy of the Erkovtsy brown coal field (the Zeya-Bureya sedimentary basin). *Stratigraphy and Geological Correlation 15*(4), 385–400.

Kezina, T.V., & Ol'kin, G.F. (2000). Palynological characteristics of Cenozoic coal-bearing deposits, the Snezhnogorskii locality in the Verkhnyaya Zeya Basin. *Stratigraphy and Geological Correlation 8*(5), 482–490.

Kharkevich, S.S. (Ed.), (1989). *Sosudistye rasteniya sovetskogo Dal'nego Vostoka* (pp. 1-380). Tom 4. Vladivostok: Nauka. [in Russian]

Kisterova, I.B., Narhinova, V.E., & Terekhova, V.E. (1979). On the issue of identifying Paleocene sediments in the north of the Chukotka Peninsula, In Yu.P Baranova, N.A. Shilo (Eds.), *Continental Tertiary strata of Northeast Asia (Stratigraphy, Correlation, Paleoclimates)* (pp. 52–55). Novosibirsk: Nauka. [in Russian]

Kodrul, T.M. (1999). *Paleogene stratigraphy of South Sakhalin* (pp.1-150). Transaction of the Geological Institute, Vol. 519. Moscow: Nauka. [in Russian]

Kottek, M., Grieser, J., Beck, C., Rudolf, B., & Rubel, F. (2006). Weltkarte der Köppen-Geiger Klimaklassifikation aktualisiert. *Meteorologische Zeitschrift 15*(3), 259–263.

Krapp, M., & Jungclaus, J.H. (2011). The middle Miocene climate as modelled in an atmosphere-ocean-biosphere madel. *Climate of the Past 7*, 1169–1188.

Krasnyi, L.I. (Ed.), (1994). *Decisions of the IV Interdepartmental Regional Stratigraphic Meeting on Precambrian and Phanerozoic in the South of the Far East and Eastern Transbaikalia* (pp. 1-124). Khabarovsk: Izdatel'stvo KhGGGP. [in Russian]

Krassilov, V.A. (1976). *Tsagayanskaya flora of the Amur Region* (pp. 1-92). Vladivostok: Nauka. [in Russian]

Krassilov, V.A. (1989). Change of flora on the border of Cretaceous and Paleogene in the Kavalerovskii District, Primorye, In V.A Krassilov, & R.S. Klimova (Eds.), *Cenozoic of the Far East* (pp. 34–37). Vladivostok: Dal'nevostochnoe otdelenie Akademii nauk SSSR. [in Russian]

Kryshtofovich, A.N. (1958). Fossil floras of Penzhinskaya Bay, Tastakh Lake and Rarytkin Ridge (pp. 73-124),. In A.L Takhtadjan, (Ed.), *Trudy BIN AN SSSR*, Seria 8, Vol. 3. Saint Petersburg: Nauka. [in Russian]

Kulkova, I.A. (1971). Eocene flora of the Yana-Indigirskaya lowland and its comparison with coeval floras of the Northern Hemisphere, In V.N. Saks, V.S. Volkova (Eds.), *Cenozoic floras of Siberia according to palynological data*. Novosibirsk: Transactions of Academy of Sciences of USSR, Siberian Branch, *135,* 34–37. [in Russian]

Kulkova, I.A. (1973). *Palynological studies of the Eocene deposits of the Yano-Indigirskaya lowland* (pp. 1-116). Novosibirsk: Nauka. [in Russian]

Kutzbach, J.E., Geutter, P.J., Ruddiman, W.F., & Prell, W.L. (1989). Sensitivity of climate to late Cenozoic uplift in southern Asia and the Amercian West: numerical experiments. *Journal of Geophysical Research: Atmospheres 94 (D15)*, 18393–18407.

Kutzbach, J.E., Prell, W.L., & Ruddiman, W.F. (1993). Sensitivity of Eurasian climate to surface uplift of the Tibetan Plateau. *Journal of Geology 101*, 177–190.

Laukhin, S.A., Akhmetiev, M.A., Fradkina, A.F., & Zyryanov, E.V. (1988). Palynological characteristics of the Kungin Paleogene of North Yakutia. *Doklady Akademii nauk SSSR 299(3)*, 686–689. [in Russian]

Li, Z.X. (1998). Eocene palynology of Well LF13-2-1 in Pearl River Mouth Basin. *China Offshore Oil and Gas (Geology) 12*, 168–173.

Li, Q.J., Utescher, T., Liu, Y.S. (Ch.), Ferguson, D., Jia, H., & Quan, C. (2022). Monsoonal climate of East Asia in Eocene times inferred from an analysis of plant functional types. *Palaeogeography, Palaeoclimatology. Palaeoecology 601*, 111138.

Licht, A., van Cappelle, M., Abels, H.A., Ladant, J.B., Trabucho-Alexandre, J., France-Lanord, C., Donnadieu, Y., Vandenberghe, J., Rigaudier, T., Lecuyer, C., Terry, D., Adriaens, R., Boura, A., Guo, Z., Soe, A.N., Quade, J., Dupont-Nivet, G., & Jaeger, J.J. (2014). Asian monsoons in a Late Eocene greenhouse world. *Nature 513*, 501–506.

Liu, T. (1997). Geological environments in China and global change, In H. Wang, B. Jahn, & S. Mei (Eds.), *Origin and History of the Earth. Proceedings of the 30th International Geological Congress, 1. VSP*, 15–26.

Liu, X.D., & Yin, Z.Y. (2002). Sensitivity of East Asian monsoon climate to the uplift of the Tibetan Plateau. *Palaeogeography, Palaeoclimatology. Palaeoecology 183*, 223–245.

Liu, J., Hertel, T.W., Diffenbaugh, N.S., Delgado, M.S., & Ashfaq, M. (2015). Future property damage from flooding: Sensetivity to economy and climate change. *Climatic Change 132*, 741–749.

Loope, D.B., Rowe, C.M., & Joeckel, R.M. (2001). Annual monsoon rains recorded by Jurassic dunes. *Nature 412*, 64–66.

Ma, Y., Tao, M., & Chen, F. (1995). The red bed sporo-pollen assemblages and geological age from Zheerzhuang of Yaojie, Gansu. *Acta Sedimentaologica Sinica 13*, 64–72.

Mamontova, I.B. (1977). Palynology of the transitional Cretatious-Paleogene beds in the Amur-Zea depression, In V.A. Krassilov (Ed.), *Paleobotany in the Far East* (pp. 32–37). Vladivostok: Far Eastern Scientific Center of the AN USSR. [in Russian]

Manchester, S.R., Crane, P.R., & Golovneva, L.B. (1999). An extinct genus with affinities to extant *Davidia* and *Camptotheca* (Cornales) from the Paleocene of North America and Eastern Asia. *International Journal of Plant Science 160*(1), 188–207.

Matthiessen, J., Knies, J., Vogt, C., & Stein, R. (2009). Pliocene palaeoceanography of the Arctic Ocean and subarctic seas. *Philosophical Transactions of the Royal Society of London A367*, 21–48.

Molnar, P., Boos, W.R., & Battisti, D.S. (2010). Orographic controls on climate and paleoclimate of Asia: thermal and mechanical roles for the Tibetan Plateau. *Annual Review of Earth and Planetary Sciences 38*, 77–102.

Moiseeva, M.G., Kodrul, T.M., & Herman, A.B. (2018). Early Paleocene Boguchan flora of the Amur Region (Russian Far East): Composition, age and palaeoclimatic implications. *Review of Palaeobotany and Palynology 253*, 15–36.

Mosbrugger, V., & Utescher, T. (1997). The coexistence approach - a method for quantitative reconstructions of Tertiary terrestrial palaeoclimate data using plant fossils. *Paleogeography, Palaeoclimatology, Palaeoecology 134*, 61–86.

Mosbrugger, V., Utescher, T., & Dilcher D. (2005). Cenozoic continental climatic evolution of Central Europe. *Proceedings of the National Academy of Sciences, 102*(42), 14964–14969.

Muling, L. (1983). The late Upper Cretaceous to Paleocene spore-pollen assemblages from the Furao area, Heilongjiang Province. *Bulletin of the Sheny and Institute of geology and mineral resources, Chinese Academy of Geological Sciences 7*, 99–137.

Müller, M.J., & Hennings, D. (2000). *The Global Climate 592 Data Atlas on CD Rom.* Flensburg: University Flensburg, Institute für Geografie.

Naryshkina, A.V. (1973). On the boundary between the Cretaceous and Paleogene deposits in the Amur-Zeya depression. *Sovetskaya Geologiya 6*, 148–151. [in Russian]

New, M., Lister, D., Hulme, M., & Makin, I. (2002). A high-resolution data set of surface climate over global land areas. *Climate Research 21*, 1–25.

Oleinikov, A.V., & Klimova, R.S. (1977). New data on stratigraphy of Neogene volcanogenic sediments of the Samarga River basin, In V.G. Varnavskii (Ed.), *Stratigraphy of the Cenozoic sediments of the Far East* (pp. 76–80). Vladivostok: Dal'nevostochnyi nauchnyi tsentr Akademii nauk SSSR. [in Russian]

Pagani, M., Zachos, J.C., Freeman, K.H., Tipple, B., & Bohany, S. (2005). Marked decline in atmospheric carbon dioxide concentrations during the Paleogene. *Science 309*, 600–603.

Parrish, J.T., Ziegler, A., & Scotese, C.R. (1982). Rainfall patterns and the distribution of coals and evaporites in the Mesozoic and Cenozoic. *Paleogeography, Palaeoclimatology, Palaeoecology 40*, 67–101.

Parthasarathy, B., Rupa Kumar, K., & Kothawale, D.R. (1992). Indian summer monsoon rainfall indices: 1871–1990. *Meteorological Magazine 121*, 174–186.

Passey, B.H., Ayliffe, L.K., Kaakinen, A., Zhang, Z.Q., Eronen, J.T., Zhu, Y.M., Zhou, L.P., Cerling, T.E., & Fortelius, M. (2009). Strengthened East Asian summer monsoons during a period of high-latitude warmth? Isotopic evidence from Mio-Pliocene fossil mammals and soil carbonates from northern China. *Earth and Planetary Science Letters 277*, 443–452.

Pavlyutkin, B.I., & Golozubov, V.V. (2010). Paleobotanic evidences for the time of the Sea of Japan origin. *Vestnik KRAUNTs, Nauki o Zemle 2*(16), 19–26. [in Russian]

Pavlyutkin, B.I., & Petrenko, T.I. (2010). *Stratigrafiya paleogen-neogenovykh otlozhenii Primor'ya* (pp.1-164 p.). Vladivostok: Dal'nauka. [in Russian]

Pearson, P.N., van Dongen, B.E., Nicholas, C.J., Pancost, R.D., Schouten, S., Singano, J.M., & Wade, B.S. (2007). Stable warm tropical climate through the Eocene Epoch. *Geology 35*, 211–214.

Pearson, P.N., Foster, G.L., & Wade, B.S. (2009). Atmospheric carbon dioxide through the Eocene–Oligocene climate transition. *Nature 461*, 1110–1113.

Pogosyan, Kh.P. (1972). *General atmospheric circulation* (pp. 1-393). Leningrad: Gidrometeoizdat. [in Russian]

Qiang, X., An, Z., Song, Y., Chang, H., Sun, Y., Liu, W., Ao, H., Dong, J., Fu, C., Wu, F., Lu, F., Cai, Y., Zhou, W., Cao, J., Xu, X., & Ai, L. (2011). New eolian red clay sequence on the western Chinese Loess Plateau linked to onset of Asian desertification about 25 Ma ago. *Science China Earth Science 54*, 136–144.

Quan, C., & Zhang, L. (2005). An analysis of the Early Paleogene climate of the Jiayin Area, Heilongjiang province. *Geological Review 51*, 10–15. [in Chinese with English abstract]

Quan, C., Liu, Y.C., & Utescher, T. (2011). Paleogene evolution of precipitation in Northeastern China supporting the Middle Eocene intensification of the East Asian Monsoon. *Palaios 26*, 743–753.

Quan, C., Liu, (Y.S.) C., & Utescher, T. (2012a). Eocene monsoon prevalence over China: A palaeobotanical perspective. *Palaeogeography, Palaeoclimatology. Palaeoecology 365-366*, 302–311.

Quan, C., Liu, (Y.S.) C., & Utescher, T. (2012b). Paleogene temperature gradient, seasonal variation and climate evolution of northeast China. *Palaeogeography, Palaeoclimatology. Palaeoecology 313-314*, 150–161.

Rhines, P.B., & Häkinnen, S. (2003). Is the oceanic heat transport in the North Atlantic irrelevant to the climate in Europe? *ASOF Newsletter 1*, 13-17.

Royer, D.L., Osborne, C.P., & Beerling, D.J. (2003). Carbon loss by deciduous trees in a CO_2-rich ancient polar environment. *Nature 424*, 60–62.

Schubert, B.A., Jahren, A.H., Eberle, J.J., Sternberg, L.S.L., & Eberth, D.A. (2012). A summertime rainy season in the Arctic forests of the Eocene. *Geology 40*, 523–526.

Scotese, C.R. (2013). *Map Folio 13, (Early Eocene, Ypresian, 52.2 Ma), PALEOMAP PaleoAtlas for ArcGIS*, volume 1, Cenozoic, PALEOMAP Project, Evanston, IL.

Sehsah, H., Furnes, H., Pham, L.T., & Eldosouky, A.M. (2022). Plume-MOR decoupling and the timing of India – Eurasia collision. *Scientific Reports 12*, 13349.

Semakin, V.P., Kochergin, A.V., & Pitina, T.I. (2016). Neotectonics of the Sea of Okhotsk. *Geodynamics and Tectonophysics 7*(2), 251–271.

Shellito, C.J., & Sloan, L.C. (2006). Reconstructing a lost Eocene paradise: Part I. Simulating the change in global floral distribution at the initial Eocene thermal maximum. *Global and Planetary Change 50*, 1–17.

Shukla, A., Mehrotra, R.C., Spicer, R.A., Spicer, T.E.V., & Kumar, M. (2014). Cool equatorial terrestrial temperatures and the South Asian monsoon in the Early Eocene: evidence from the Gurha Mine, Rajasthan, India. *Palaeogeography, Palaeoclimatology. Palaeoecology 412*, 187–198.

Smith, R.Y., Basinger, J.F., & Greenwood, D.R. (2012). Early Eocene plant diversity and dynamics in the Falkland flora, Okanagan Highlands, British Columbia, Canada. *Palaeobiodiversity and Palaeoenvironments 92*(3), 309–328.

Sokolov, S., Svjseva, O., & Kubli, V. (1977). *Ranges of trees and shrubs of the USSR*, Volume 1. Leningrad: Nauka. [in Russian]

Sokolov, S., Svjseva, O., & Kubli, V. (1980). *Ranges of trees and shrubs of the USSR*, Volume 2. Leningrad: Nauka. [in Russian]

Sokolov, S., Svjseva, O., & Kubli, V. (1986). *Ranges of trees and shrubs of the USSR*, Volume 3. Leningrad: Nauka. [in Russian]

Song, Z.C., & Zhang, D.H. (1990). Geological age of the Caomuhao gypsum mine in Oto Banner, Nei Mongol with review of research on fossil proteaceous pollen in China. *Acta Palaeobotanica Sinica 29*, 257–269.

Sorokin, A.P., & Belousov, V.I. (1984). Cenozoic of the western part of the Urkanskii Basin, In A.G. Ablaev (Ed.), *Materials on stratigraphy and paleogeography of East Asia (new data)* (pp. 48–52). Vladivostok: Far Eastern Scientific Center of the AN USSR. [in Russian]

Spicer, R.A., & Corfield, R.M. (1992). A review of terrestrial and marine climates in the Cretaceous and implications for modelling the greenhouse earth. *Geological Magazine 129*, 168–180.

Spicer, R.A., & Herman, A.B. (2010). The Late Cretaceous environment of the Arctic: a quantitative reassessment using plant fossils. *Palaeogeography, Palaeoclimatology, Palaeoecology 295*, 423–442.

Spicer, R.A., & Parrish, J.T. (1986). Paleobotanical evidence for cool North Polar climates in middle Cretaceous (Albian-Cenomanian) time. *Geology 14*, 703–706.

Spicer, R.A., Herman, A.B., Liao,W., Spicer, T.E.V., Kodrul, T., Yang, J., & Jin, J. (2014). Cool tropics in the Middle Eocene: evidence from the Changchang Flora, Hainan Island, China. *Palaeogeography Palaeoclimatology Palaeoecology 412*, 1–16.

Spicer, R.A., Yang, J., Herman, A.B., Kodrul, T., Maslova, N., Spicer, T.E.V., Aleksandrova, G.N., & Jin, J.H. (2016). Asian Eocene monsoons as revealed by leaf architectural signatures. *Earth and Planetary Science Letters 449*, 61–68.

Spicer, R.A., Yang, J., Herman, A., Kodrul, T., Aleksandrova, G., Maslova, N., Spicer, T.E.V., Ding, L., Xu, Q., Shukla, A., Srivastava, G., Mehrotra, R.C., & Jin, J.H. (2017). Paleogene monsoons across India and South China: drivers of biotic change. *Gondwana Research 49*, 350–363.

Spicer, R.A., Valdes, P., Hughes, A., Yang, J., Spicer, T., Herman, A., & Farnsworth, A. (2019). New insights into the thermal regime and hydrodynamics of the early Late Cretaceous Arctic. *Geological Magazine 157*, 1729–1746.

Spicer, R.A., Su, T., Valdes, P.J., Farnsworth, A., Wu, F.X., Shi, G., Spicer, T.E.V., & Zhou, Z.K. (2021). Why 'the uplift of the Tibetan Plateau' is a myth. *National Science Review 8(1)*, nwaa091.

Srivastava, G., Spicer, R.A., Spicer, T.E.V., Yang, J., Kumar, M., Mehrotra, R.C., & Mehrotra, N.C. (2012). Megaflora and palaeoclimate of a Late Oligocene tropical delta, Makum Coalfield, Assam: evidence for the early development of the South Asia Monsoon. *Palaeogeography, Palaeoclimatology, Palaeoecology 342-343*, 130–142.

Su, T., Xing, Y.W., Yang, Q.S., & Zhou, Z.K. (2009). Reconstructions of mean annual temperature in Chinese Eocene Paleofloras based on leaf margin analysis. *Acta Palaeontologica Sinica 48*, 65–72.

Suan, G., Popescu, S.-M., Suc, J.-P., Schnyder, J., Fauquette, S., Baudin, F., Yoon, D., Piepjohn, K., Sobolev, N.N., & Labrousse, L. (2017). Subtropical climate conditions and mangrove growth in Arctic Siberia during the early Eocene. *Geology 45*, 539–542.

Sun, X.J., & Wang, P. (2005). How old is the Asian monsoon system? – palaeobotanical records from China. *Palaeogeography, Palaeoclimatology. Palaeoecology 222*, 181–222.

Sun, X.Y., Zhao, Y.N., & He, Z.S. (1980). Late Cretaceous–Early Tertiary pollen assemblages in Xining–Minhe Basin and its geological age, paleovegitational, and paleoclimatic significance. *Experimental Petroleum Geology 2*, 44–50.

Sycheva, O.A. (1975). On the flora and age of the Kama layers of the Boshnyakovskaya Formation of the Uglegorsky District of Sakhalin Island, In L.S. Zhidkova (Ed.), *Stratigraphy, lithology and paleogeography of the Meso-Cenozoic deposits of the Far East* (pp. 13–18). Vladivostok: Proceedings of the SakhKNII, vol. 36. Far Eastern Scientific Center of the AN USSR. [in Russian]

Takaya, K., & Nakamura, H. (2005). Mechanisms of intraseasonal amplification of the cold Siberian High. *Journal of Atmospheric Sciences 62*, 4423–4440.

Tanai, T. (1972). Tertiary history of vegetation in Japan, In A. Graham (Ed.), *Floristics and Paleofloristics of Asia and Eastern North America* (pp. 234–255). Proceedings of Symposia for the Systematics Section, XI International Botanical Congress, Seattle, Wash. 1969, and The Japan-United States Cooperative Science Program, Corvallis, Oregon 1969. Elsevier Publishing Company.

Tao, J.R., & Xiong, X.Z. (1986). The latest Cretaceous flora of Heilongjiang Province and the floristic relationship between East Asia and North America. *Acta Phytotaxonomica Sinica 24*(1), 1–15.

Tashchi, S.M., Ablaev, A.G., & Mel'nikov, N.G. (1996). *Cenozoic basin of the Western Primorye and adjacent territories of China and Korea* (pp. 1-168). Vladivostok: Dal'nauka. [in Russian]

Uhl, D., Traiser, C., Griesser, U., & Denk, T. (2007). Fossil leaves as palaeoclimate proxies in the Palaeogene of Spitsbergen (Svalbard). *Acta Palaeobotanica Krakow 47(1)*, 89–107.

Utescher, T., & Mosbrugger, V. (2018). The Palaeoflora Database. Available at www.palaeoflora.de (last accessed 08 August 2020).

Utescher, T., Mosbrugger, V., Bruch, A.A., & Milutinovic, D. (2007). Climate and vegetation changes in Serbia during the last 30 Ma. *Palaeogeography, Palaeoclimatology, Palaeoecology 253*, 141–152.

Utescher, T., Bruch, A.A., Micheels, A., Mosbrugger, V., & Popova, S. (2011). Cenozoic climate gradients in Eurasia a palaeo-perspective on future climate change? *Palaeogeography, Palaeoclimatology, Palaeoecology 304*, 351–358.

Utescher, T., Bruch, A.A., Erdei, B., François, L., Ivanov, D., Jacques, F.M.B., Kern, A.K., Liu, (Y.-S.) C., Mosbrugger, V., & Spicer, R.A. (2014). The Coexistence Approach – Theoretical background and practical considerations of using plant fossils for climate 666 quantification. *Palaeogeography, Palaeoclimatology, Palaeoecology 410*, 58–73.

Utescher, T., Bondarenko, O.V., & Mosbrugger, V. (2015). The Cenozoic Cooling – continental signals from the Atlantic and Pacific side of Eurasia. *Earth and Planetary Science Letters 415*, 121–133.

Van Beuskom, C.F. (1971). Revision of *Meliosma* (Sabiaceae) section Lorenzanea excepted, living and fossil, geography and phylogeny. *Blumea 19*, 355–529.

Varnavskii, V.G., Sedykh, A.K., & Rybalko, V.I. (1988). *Paleogene and Neogene of the Amur Region and Primorye* (pp. 1-184). Vladivostok: Izdatel'stvo DVO AN SSSR. [in Russian]

Verkhovskaya, N.B., & Kundyshev, A.S. (1989). Physiognomic features of spore-pollen spectra and their use in stratigraphy, In V.A. Krassilov, R.S. Klimova (Eds.), *Cenozoic of the Far East* (pp. 128–134). Vladivostok: Dal'nevostochnoe otdelenie Akademii nauk SSSR. [in Russian]

Volkova, V.S., & Kuz'mina, O.B. (2005). Flora, vegetation, and climate of the middle Cenophytic (Paleocene – Eocene) of Siberia. *Geologia i geofizika 46(8)*, 844–855. [in Russian]

Volobueva, V.I., Gladenkov, Yu.B., & Belaya, B.V. (1988). Paleogene of the Northeastern USSR. In V.P Pokhialainen, & M.Kh. Gagiev (Eds.), *Stratigrafiya i paleontologiya fanerozoya Severo-Vostoka SSSR* (pp. 118–156). Magadan: Izdatel'stvo SVKNII DVO AN SSSR. [in Russian]

Wan, S.M., Li, A.C., Clift, P.D., & Stuut, J.W. (2007). Development of the East Asian monsoon: mineralogical and sedimentologic records in the northern South China Sea since 20 Ma. *Palaeogeography, Palaeoclimatology, Palaeoecology 254*, 561–582.

Wang, X.M. (2005). Eocene palynostratigraphy of Wutu, Shandong and its stratigraphical significance. *Journal of Stratigraphy 29*, 22–27.

Wang, P. (2009). Global monsoon in a geological perspective. *Chinese Science Bulletin 54*, 1–24.

Wang, B., & Fan, Z. (1999). Choice of south Asian summer monsoon indices. *Bulletin of the American Meteorological Society 80*, 629–638.

Wang, J.Y., & Wang, D.F. (1982). Age determination by K–Ar method for the bottom of the Palaeocene Laohutai Formation at Fushun district. *Bulletin of the Geological Society of Liaoning Province 1*, 110–115. [in Chinese, with English abstract]

Wang, J.Y., & Wang, D.F. (1985). Age determination of basalt of Palaeocene Laohutai Formation in Fushun district by delation method of K–Ar elements. *Bulletin of the Geological Society of Liaoning Province 1*, 86–90. [in Chinese, with English abstract]

Wang, D.N., & Zhao, Y.N. (1980). Late Cretaceous–Early Paleogene sporopollen assemblages of the Jianghan Basin and their stratigraphical significance. *Professional Paper of Chinese Academy of Geological Sciences (Stratigraphy and Palaeontology) 9*, 1–174.

Wang, D.F., Gao, R.F., Wang, J.Y., & Fan, Y.Q. (1982). Paleomagnetic determination for lower limits of Early Cretaceous and Palaeocene systems in Liaoning. *Bulletin of the Geological Society of Liaoning Province 1*, 116–121. [in Chinese, with English abstract]

Wang, D.N., Sun, X.Y., & Zhao, Y.N. (1984). The Paleocene – Eocene palynoflora from the Tantou Basin in west Henan. *Acta Botanica Sinica 26*, 448–455.

Wang, D.N., Sun, X.Y., & Zhao, Y.N. (1986). Palynoflora from Late Cretaceous to Tertiary in Qinghai and Xinjiang. *Bulletin of the Institute of Geology, Chinese Academy of Geological Sciences 15*, 152–169.

Wang, K.F., Zhang, Y.L., & Wang, R. (1987). *Cretaceous–Tertiary Palynological assamblages from Anhui*. Beijing: Petroleum Industry Press.

Wang, J., Wang, Y.J., Liu, Z.C., Li, J.Q., & Xi, P. (1999). Cenozoic environmental evolution of the QaidamBasin and its implications for the uplift of the Tibetan Plateau and the drying of central Asia. *Palaeogeography, Palaeoclimatology, Palaeoecology 152*, 37–47.

Wang, Q., Ferguson, D.K., Feng, G.P., Ablaev, A.G., Wang, Y.F., Yang, J., Li, Y.L., & Li, C.S. (2010). Climatic change during the Palaeocene to Eocene based on fossil plants from Fushun, China. *Palaeogeography, Palaeoclimatology, Palaeoecology 295*, 323–331.

West, C.K., Greenwood, D.R., & Basinger, J.F. (2015). Was the Arctic Eocene 'rainforest' monsoonal? Estimates of seasonal precipitation from early Eocene megafloras from Ellesmere Island, Nunavut. *Earth and Planetary Science Letters 427*, 18–30.

West, C.K., Greenwood, D.R., Reichgelt, T., Lowe, A.J., Vachon, J.M., & Basinger, J.F. (2020). Paleobotanical proxies for early Eocene climates and ecosystems in North America from middle to high latitude. *Climate of the Past 16*, 1387–1410.

Westerhold, T., Marwan, N., Drury, A.J., Liebrand, D., Agnini, C., Anagnostou, E., Barnet, J.S.K., Bohaty, S.M., De Vleeschouwer, D., Florindo, F., Frederichs, T., Hodell, D.A., Holbourn, A., Kroon, D., Lauretano, V., Littler, K., Lourens, L.J., Lyle, M.W., Pälike, H., Röhl, U., Tian, J., Wilkens, R.H., Wilson, P.A., & Zachos, J.C. (2020). An astronomically dated record of Earth's climate and its predictability over the last 66 million years. *Science 369*, 1383–1387.

Wilf, P. (2000). Late Paleocene-early Eocene climate changes in southwestern Wyoming: paleobotanical analysis. *Geological Society of America Bulletin 112*, 292–307.

Wing, S.L. (1998). Tertiary vegetation of North America as a context for mammalian evolution. In C.M. Janis, K.M. Scott, L.L. Jacobs, G.F Gunnell, & M.D. Uhen (Eds.), *Evolution of Tertiary Mammals of North America* (pp. 37–65). Cambridge University Press.

Wing, S.L., & Greenwood, D.R. (1993). Fossils and fossil climate: the case for equable continental interiors in the Eocene. *Philosophical Transactions of the Royal Society, B: Biological Sciences 341*, 243–252.

Wing, S.L., & Harrington, G.J. (2001). Floral response to rapid warming in the earliest Eocene and implications for concurrent faunal change. *Paleobiology 27*, 539–563.

Wing, S.L., Harrington, G.J., Smith, F.A., Bloch, J.I., Boyer, D.M., & Freeman, K.H. (2005). Transient floral change and rapid global warming at the Paleocene–Eocene boundary. *Science 310*, 993–996.

Wolfe, J.A. (1978). A paleobotanical interpretation of Tertiary climates in the Northern Hemisphere. *American Scientist 66*, 694–703.

Wolfe, J.A. (1994). Tertiary climatic changes at middle latitudes of western North America. *Palaeogeography, Palaeoclimatology, Palaeoecology 108*, 195–205.

Wolfe, J.A. (1995). Paleoclimatic estimates from Tertiary leaf assemblages. *Annual Review of Earth and Planetary Sciences 23*, 119–142.

Wu, Z.Y., & Raven, P.H. (Eds.), (1999). *Flora of China* (pp. 1-453). vol. 4 (Cycadaceae through Fagaceae). Science Press, Beijing and Missouri Botanical Garden.

Xiao, G.Q., Abels, H.A., Yao, Z., Dupont-Nivet, G., & Hilgen, F.J. (2010). Asian aridification linked to the first step of the Eocene–Oligocene climate Transition (EOT) in obliquity-dominated terrestrial records (Xining Basin, China). *Climate of the Past 6*, 501–513.

Xing, Y., Utescher, T., Jacques, F.M.B., Su, T., Liu, Y., Huang, Y., & Zhou, Z. (2012). Paleoclimatic estimation reveals a weak winter monsoon in southwestern China during the late Miocene: evidence from plant macrofossils. *Palaeogeography, Palaeoclimatology, Palaeoecology 358-360*, 19–26.

Yao, Y.F., Bera, S., Ferguson, D.K., Mosbrugger, V., Paudayal, K.N., Jin, J.H., & Li, C.S. (2009). Reconstruction of paleovegetation and paleoclimate in the early and middle Eocene, Hainan Island, China. *Climatic Change 92*, 169–189.

Zachos, J.C., Dickens, G.R., & Zeebe, R.E. (2008). An early Cenozoic perspective on greenhouse warming and carbon-cycle dynamics. *Nature 451*, 279–283.

Zaklinskaya, E.D. (1976). Key and correlative taxa and palynological correlation of sediments bordering between the Mesozoic and Cenozoic systems in South Sakhalin, In A.G. Ablaev (Ed.), *Essays on the geology and paleontology of the Far East* (pp. 51–65). Vladivostok: Far Eastern Scientific Center of the Academy of Sciences of the USSR. [in Russian]

Zaklinskaya, E.D., Brattseva, G.M., & Krassilov, V.A. (1977). On the palynoflora of the Tsagaian stratotype, In V.A. Krassilov (Ed.), *Paleobotany in the Far East* (pp. 28–31). Vladivostok: Far Eastern Scientific Center of the AN USSR. [in Russian]

Zhang, T., & Yin, F. (2005). Sporopollen assemblages from the Shahejie Formation in the Tanbai area of Huanghua depression. *Journal of Northwest University (Natural Science Edition) 35*, 91–94.

Zhang, Q., Willems, H., Ding, L., Gräfe, K.U., & Appel, E. (2012). Initial India–Asia continental collision and foreland basin evolution in the Tethyan Himalaya of Tibet: evidence from stratigraphy and paleontology. *Journal of Geology 120*, 175–189.

Zhang, Q.-Q., Smith, T., Yang, J., & Li, C.-S. (2016). Evidence of a Cooler Continental Climate in East China during the Warm Early Cenozoic. *PLoS ONE 11(5)*, e0155507.

Zhang, S., & Wang, B. (2008). Global summer monsoon rainy seasons. *International Journal of Climatology 28*, 1563–1578.

Zhang, Y.Y., & Qian, Z.S. (1992). Eocene palynofloras from the Dainan and Sanduo formations in north Jiangsu with special reference to Eocene climatic changes in southeast China. *Acta Micropalaeontologica Sinica 9*, 1–24.

Zhang, Y.Y., Wang, K.D., Liu, J.L., & Zheng, Y.H. (1990). Eocene palynoflora from the southwestern continental shelf basin of the East China Sea. *Acta Micropalaeontologica Sinica 7*, 389–402.

Zhang, Z., Wang, H., Guo, Z., & Jiang, D. (2007). What triggers the transition of palaeoenvironmental patterns in China, the Tibetan

Plateau uplift or the Paratethys Sea retreat? *Palaeogeography, Palaeoclimatology, Palaeoecology 245*, 317–331.

Zhang, Z., Flatoy, F., Wang, H., Bethke, I., Bentsen, M., & Guo, Z. (2012). Early Eocene Asian climate dominated by desert and steppe with limited monsoons. *Journal of Asian Earth Sciences 44*, 24–35.

Zhao, P., Zhou, X.J., Chen, L.X., & He, J.H. (2009). Characteristics of subtropical monsoon and rainfall over Eastern China and Western North Pacific. *Acta Meteorologica Sinica 23*, 649–665.

Zharikova, L.P. (1980). Paleogene spore-pollen complexes of the right bank of the Kolyma River, In V.F Vozin (Ed.), *Cenozoic of Eastern Yakutia* (pp. 18–35). Yakutsk: Yakut Branch of the Siberian Department of the USSR Akademy of Sciences. [in Russian]

Zharikova, L.P., Kazantsev, A.S., Minyuk, P.S., & Savcheshu, A.G. (1982). New data on the stratigraphy of the eastern part of the Primorskaya lowland, In V.B. Spektor (Ed.), *Geology of the Cenozoic of Yakutia* (pp. 28–34). Yakutsk: Yakut Branch of the Siberian Department of the USSR Akademy of Sciences. [in Russian]

Zhou, T. (1984). *Chinese Natural Geography*. Paleogeography 1. Beijing: Science. [in Chinese]

Ziegler, M., Tuenter, E., & Lourens, L.J. (2010). The precession phase of the boreal summer monsoon as viewed from the eastern Mediterranean (ODP site 968). *Quaternary Science Reviews 29*, 1481–1490.

Ziva, M.V. (1973). Palynological characteristics of the Paleogene deposits of the Amur-Zeya Depression, In E.D. Zaklinskaya (Ed.), *Palynologiya kainofita* (pp. 89–93). (Proceedings of the Third International Palynological Conference). Moscow: Nauka. [in Russian]

Ziva, M.V., & Lukashova, L.I. (1977). Palynological characteristics of the Paleogene and Neogene deposits of the Middle Amur depression, In V.G. Varnavskii (Ed.), *Stratigraphy of the Cenozoic sediments of the Far East* (pp. 42–47). Vladivostok: Dal'nevostochnyi nauchnyi tsentr Akademii nauk SSSR. [in Russian]